Low-complexity channel estimation for LTE-based systems in time-varying channels

by

Ahmad El-Qurneh

Bachelor of Communication Engineering,

Princess Sumaya University for Technology, 2011.

A Thesis Submitted in Partial Fulfillment
of the Requirements for the Degree of

Master of Science in Engineering

in the Graduate Academic Unit of Electrical and Computer Engineering

Supervisor:	Brent R. Petersen, Ph.D., Electrical and Comp. Eng.
Examining Board:	Maryhelen Stevenson, Ph.D., Electrical and Comp. Eng., Chair
	Julian Meng, Ph.D., Electrical and Comp. Eng.
	Yevgen Biletskiy, Ph.D., Electrical and Comp. Eng.
	Michael Fleming, Ph.D., Faculty of Comp. Science

This thesis is accepted by the

Dean of Graduate Studies

THE UNIVERSITY OF NEW BRUNSWICK

May, 2013

To my parents for their endless love and support

Abstract

For its key role in achieving high data rates, the need to develop a low-complexity channel estimator is one of the main targets in the Long-Term Evolution (LTE) research development. With high-mobility users in LTE-Orthogonal Frequency Division Multiplexing (LTE-OFDM) systems, channel estimator design becomes a challenging problem, since the estimator needs to estimate more channel parameters than in slow fading channels, which may make the channel estimation impractical.

A low-complexity channel estimator is developed for LTE high-mobility systems based on the Piecewise Linear (PWL) model and the channel time-frequency correlation relationships. The channel estimator and interpolator is tested under different LTE channel models for various mobile velocities and showed an improvement in the Bit Error Rate (BER) performance from 6% to 2% compared to the conventional linear interpolation technique with only 33.2% increase in the required processing time for a doppler frequency of 300 Hz.

The proposed interpolation technique is insensitive to the change in the mobile velocity to some extent; this makes the channel estimator more practical and robust to any change in the channel statistics.

Acknowledgment

I owe sincere gratitude and appreciation to my supervisor, Dr. Brent Petersen, for his invaluable support throughout my research work and his guidance and assistance whenever the research faced an obstacle.

I am grateful for his personal time throughout the writing of the thesis and his determination in helping me improve my English writing skills.

I offer my thanks to Shelley Cormier from the ECE administrative staff for her kindness and continuous assistance.

Lastly, I thank my family, friends and the tennis community of Fredericton for their moral support. This thesis would not have been possible without their encouragement.

Table of contents

List of figures

List of tables

List of abbreviations

LTE	Long Term Evolution
OFDM	Orthogonal Frequency Division Multiplexing
BER	Bit Error Rate
3GPP	Third Generation Partnership Project
OFDMA	Orthogonal Frequency Division Multiple Access
MIMO	Multiple Input Multiple Output
SNRs	Signal-to-Noise Ratios
ICI	Inter-Carrier Interference
PSAM	Pilot Symbol Assisted Modulation
DFT	Discrete Fourier Transform
BEM	Basis Expansion Model
CE-BEM	Complex Exponential Basis Expansion Model
P-BEM	Polynomial Basis Expansion Model
2D	Two-Dimensional
SC-FDMA	Single Carrier-Frequency Division Multiple Access
CP	Cyclic Prefix
QAM	Quadrature Amplitude Modulation

IFFT	Inverse Fast Fourier Transform
FFT	Fast Fourier Transform
RE	Resource Element
RB	Resource Block
APP	A Posterior Probability
EPA	Extended Pedestrian A
EVA	Extended Vehicular A
ETU	Extended Typical Urban
RMS	Root Mean Square
LS	Least Square
MMSE	Minimum Mean Square Error
PWL	Piecewise Linear
AWGN	Additive White Gaussian noise

Chapter 1

Introduction

1.1 Background and literature review

Wireless communication is a rapidly growing technology. The beginning of mobile communication technologies goes back to the first analog mobile radio systems, which are labelled as the first generation (1G). The second generation (2G) introduced the first digital mobile systems, while the third generation (3G) presented the first mobile systems handling broadband data transfer.

Long Term Evolution (LTE) "release 8.0" is often called the fourth generation (4G) but many claim that LTE "release 10.0", also known as LTE-Advanced, is the true 4G evolution step, while LTE "release 8.0" is referred to as 3.9G [19].

The Third Generation Partnership Project (3GPP) set up its own set of technical requirements for LTE and LTE-Advanced that includes the incorporation of many of the latest wireless communication technologies such as: Orthogonal Frequency Division multiple Access (OFDMA), Multiple Input Multiple Output (MIMO), dynamic resource allocation, channel width flexibility and mobility management [19].

The evolution into the 4G systems is driven by many factors such as: the development of new services for mobile devices and the increasing demand for higher data rates and lower latency for many interactive services.

LTE with its latest technologies promises a set of advantages for future mobile communication systems such as:

1. increased data rates,
2. support of high mobility,
3. scalable channel bandwidths,
4. improved spectral efficiency, throughput and access efficiency,
5. lower latency,
6. compatibility to existing networks and
7. multiple antenna techniques to improve the system capacity.

In this thesis, we investigate a critical part of the LTE-based receivers that contributes significantly in achieving the LTE requirements for an acceptable overall performance; this part is the channel estimation and interpolation stage.

Accurate channel estimates at the receiver have a major impact on the whole system performance. Part of the system design requires identifying low-complexity estimators that make their implementation at the receivers practical while maintaining a satisfactory Bit Error Rate (BER) performance. LTE is a promising mobile wireless communication standard that specifies high data rates to be met by high-mobility receivers. Such a specification requires many complex operations to take place in the receivers, making their implementation challenging.

Realizing low-complexity estimators in LTE-based receivers that can sustain high performance in high-mobility environments is a growing research field, where tradeoffs between complexity and BER have to be considered [1].

The support of high mobility is essential in LTE-based systems, which leads the research to focus on achieving good BER performance under fast time-varying channel environments. The signal at the receiver is distorted due to the fast time-varying channel, and the need arises for a reliable channel estimation and equalization to compensate for the distortion of the channel before the coherent detection of the received signals.

There is much on-going research in channel estimation procedures in LTE-based receivers, but most of it considers the channel as time-invariant over one or two OFDM symbols [3, 14] that makes the estimation process less computationally complex, but dramatically degrades the performance at high mobile speeds or low Signal-to-Noise Ratios (SNRs).

When the channel varies significantly over one OFDM symbol block, the orthogonality among the OFDM subcarriers is lost and Inter-Carrier Interference (ICI) is created which makes the time-invariant assumption inaccurate. ICI increases the number of channel states that need to be estimated for sufficient data estimation and detection; therefore, to reduce the number of unknown channel parameters, simplification approaches are exploited for channel estimation.

To reduce the complexity of receivers, normally the channel estimation and data decoding processes are separated, where Pilot Symbol Assisted Modulation (PSAM) is used to obtain the initial channel estimation at pilot tones and then interpolation is applied to get the full channel matrix of the data symbols [5]. Once the channel estimation step is performed, the gain and phase compensation stage is applied to compensate for the channel distortion at the data symbols. The data is decoded iteratively after that using the turbo decoder until obtaining the best possible estimate of the transmitted data.

Most of ongoing research on PSAM focuses on developing different interpolation algorithms to obtain the channel estimates at the data symbols from the known channel estimates at the pilot symbols [28].

Various interpolation techniques can be considered that vary in their computational complexity and accuracy such as: linear interpolation, second order interpolation, cubic spline, polynomial interpolation and Discrete Fourier Transform (DFT)-based interpolation. Another more complex approach is to model the channel states by one of the Basis Expansion Models (BEM) such as the Complex Exponential BEM (CE-BEM) and Polynomial BEM (P-BEM) [4].

On the other hand a different approach, which might be used in fast varying environments to get more accurate estimates and preserve low BERs, is joint channel estimation and data decoding [6, 7], which is recently receiving attention in OFDM systems.

Two-dimensional (2D) channel estimation has to be applied in LTE-based receivers, since the downlink pilot symbols are inserted in both the time and the frequency domain, but the use of the one 2D channel estimator is not practical due to its large implementation complexity, thus, interpolation with two separate one dimensional channel estimators that perform independently in time and frequency is preferred more in LTE-based receivers to reduce the implementation complexity [1].

This thesis investigates the realizing of a low-complexity channel estimator and an interpolator in fast time-varying LTE channel models. Such an estimator promises low processing time and enhanced BER performance, which in consequence makes its implementation in LTE-based receivers more practical. The motivation behind this thesis work came from the rapid development of wireless communication technologies and the need to create algorithms and techniques that achieve the requirements of the newly emerged mobile communication systems.

LTE with its promising technology is a great step in the development of wireless systems. Having such low-complexity channel estimators based on this standard supports the development process and boosts the implementation of practical receivers compatible with this standard.

1.2 Thesis contribution

The main contribution of this thesis work is the developing of a low-complexity channel estimator and interpolator in fast time-varying channels under the LTE environment, without affecting the bandwidth efficiency, while enhancing the BER performance and achieving high data rates and low processing time.

Minimizing the number of operations to be performed by the estimator to realize fast signal processing while maintaining the performance according to LTE standards is also one of the main contributions of this research.

Another major contribution is that the low-complexity channel estimator is developed for high-mobility systems and it is insensitive to the change in the mobile velocity to some extent, which makes the estimator more robust in practical systems.

1.3 Thesis structure

The remainder of this thesis consists of four chapters. Chapter 2 gives an overview of the LTE downlink system under research including the major parts of the system and the frame structure used in this thesis. Chapter 3 describes the implementation of the LTE downlink system used in simulation in Simulink® with the description of the significance of each stage. Chapter 4 discusses the proposed interpolation method in detail and gives solutions for various scenarios; it also provides an overview of the common channel estimation methods. Chapter 5 provides the results of different simulation tests and comparisons among different interpolation methods. Chapter 6 summarizes the proposed work and gives an insight for possible future research.

Chapter 2

Overview of LTE downlink physical layer transmission

2.1 Introduction

The main technologies in LTE systems are OFDM in the downlink and Single Carrier-Frequency Division Multiple Access (SC-FDMA) in the uplink transmission. Turbo coding and decoding are also used, while Multiple Input Multiple Output (MIMO) is considered for increasing system capacity by having different modes in which the LTE system can operate [2].

LTE supports high data rates, which can reach up to 100 Mbps for the downlink transmission and 50 Mbps for the uplink transmission when two antennas are used in the base station and one in the mobile station with a channel bandwidth of 20 MHz.

One key feature of LTE systems is the support of a scalable channel bandwidth that ranges from 1.4 MHz up to 20 MHz, which makes its implementation more feasible to the service providers.

2.2 OFDM implementation in downlink transmission

OFDM is a multicarrier transmission technique that is used as the LTE downlink transmission scheme. In OFDM, the wide band frequency carrier is divided into narrow band subcarriers orthogonal to each other as in figure 2.1. This orthogonality in combination with an appropriate choice of subcarrier spacing (Δf) and the Cyclic Prefix (CP) length makes the OFDM system a robust transmission technique for frequency selective channels. The wide band frequency selective channel is converted into a group of narrow band flat fading channels at each subcarrier. Each subcarrier is modulated using one of the Quadrature Amplitude Modulation (QAM) schemes suggested by the LTE standards [20], which are: 4-QAM, 16-QAM and 64-QAM.

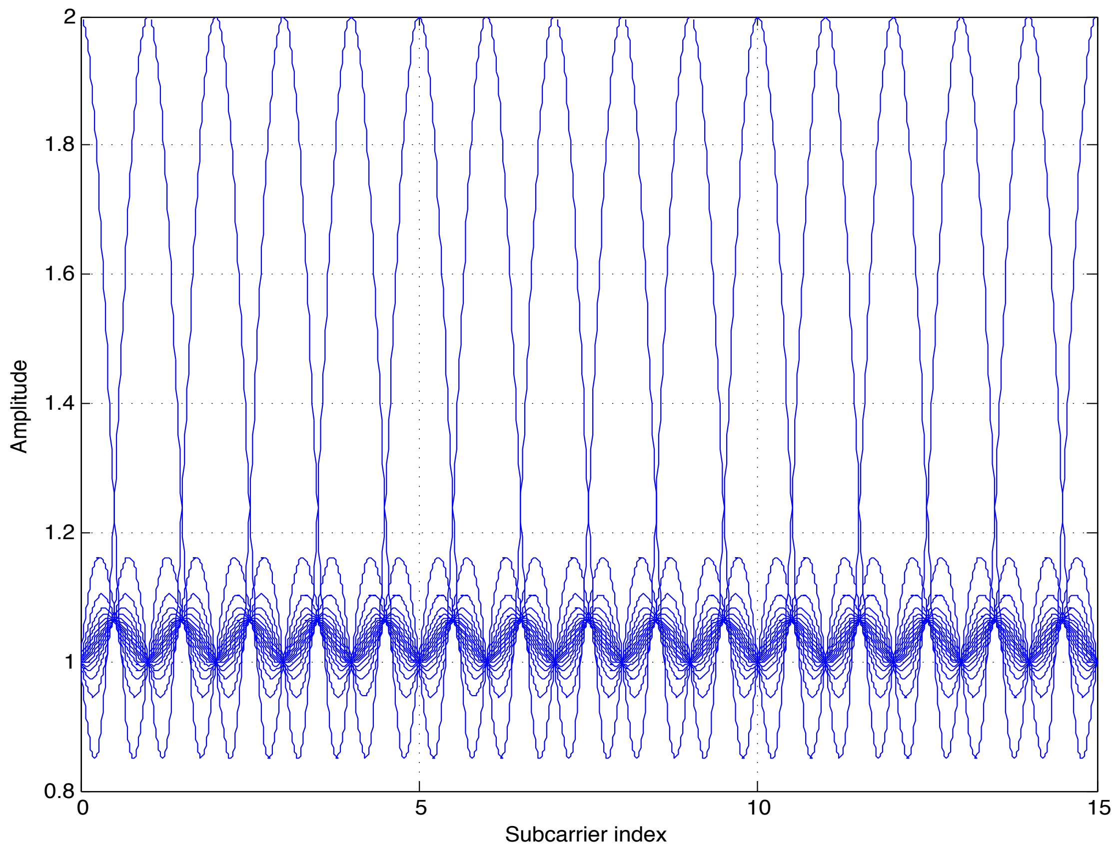

Figure 2.1: Basic OFDM subcarriers transmission

The OFDM modulator at the transmitter side is implemented using an N-point Inverse Fast Fourier Transform (IFFT) operation, where N denotes the total number of subcarriers. Using an IFFT reduces the implementation complexity significantly compared to using a bank of modulators for each subcarrier.

Each OFDM symbol in an LTE transmission frame consists of N subcarriers in the frequency domain with a frequency spacing Δf between each consecutive subcarrier. The choice of the proper Δf depends on the frequency selectivity of the channel and the maximum rate of channel variation, and the choice of the number of subcarriers depends on the assumed overall transmission bandwidth [21].

Not maintaining cyclic convolution for the OFDM subcarriers may lead to a loss of the subcarriers' orthogonality, which results in interference between adjacent subcarriers. To avoid that situation, an appropriate CP length is used. CP samples are chosen from the last part of the OFDM symbol, where a number of samples are copied and inserted at the beginning of the OFDM symbol.

In LTE-OFDM based systems, the CP has two types: normal and long. The CP's length varies depending on the channel bandwidth used and the number of OFDM symbols as shown in table 2.1.

At the receiver side, the OFDM demodulator is implemented using an N-point Fast Fourier Transform (FFT) operation to convert the signal back to the frequency domain after removing the CP.

2.3 LTE downlink frame structure

The downlink transmission frame period in LTE is 10 ms [20]; it consists of ten subframes, each one has a period of 1 ms, and each subframe consists of two slots of 0.5 ms each as shown in figure 2.2.

The slot in the time domain consists of seven OFDM symbols for the normal CP or six OFDM symbols for the long CP.

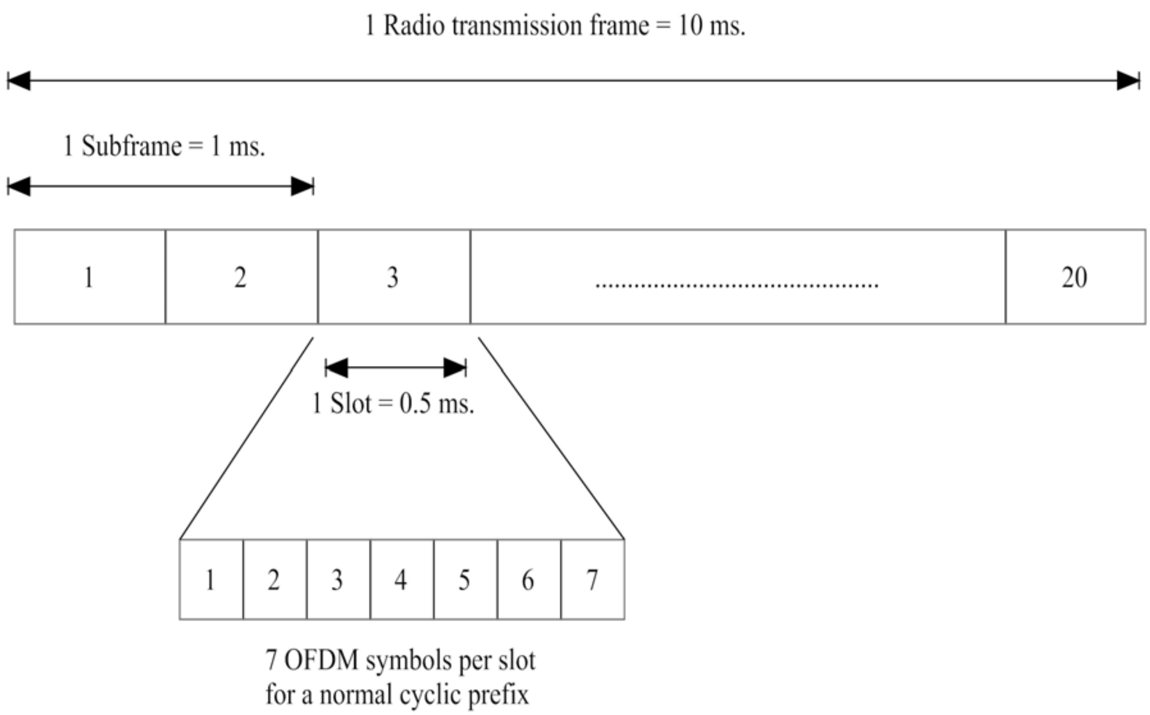

Figure 2.2: LTE downlink transmission frame structure

Each OFDM symbol in the frequency domain consists of N subcarriers with Δf being 15 kHz or 7.5 kHz between consecutive subcarriers. The smallest modulation structure in the LTE transmission frame is one symbol by one subcarrier, which is called a Resource Element (RE).

Each of the 12 subcarriers in the frequency domain with seven or six OFDM symbols in the time domain are labelled as one Resource Block (RB). Figure 2.3 shows the LTE slot structure for one RB used in the simulation model [20].

The number of RBs depends on the transmission bandwidth used, since the number of RBs in combination with the subcarrier frequency spacing determine the overall signal bandwidth [17].

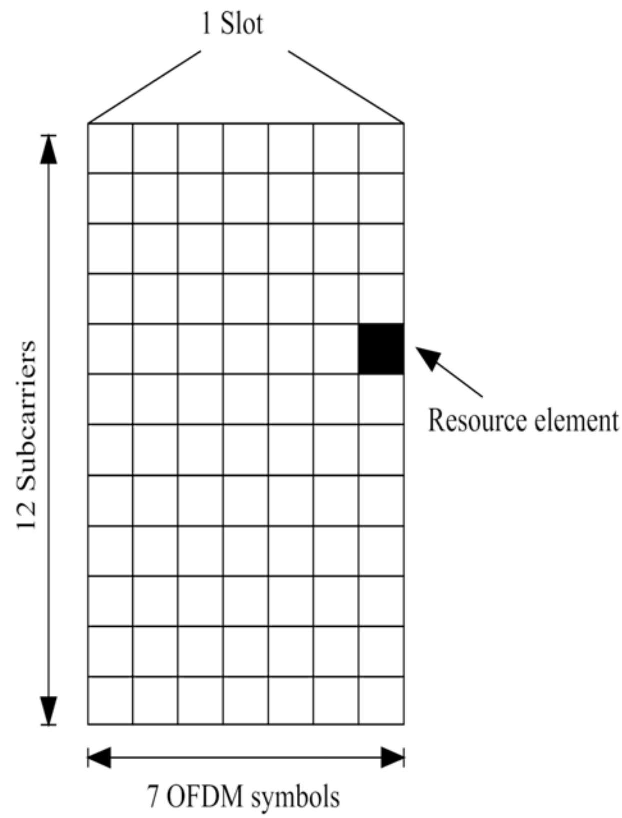

Figure 2.3: One RB structure in LTE downlink slot

2.4 OFDM parameters selection in LTE

Choosing the size of the FFT/IFFT used in the OFDM transmission depends on the channel bandwidth used as shown in table 2.1. One key point to notice here is that the CP length for the first OFDM symbol in a slot is longer than the length of the CP for the remaining OFDM symbols; the number between brackets in table 2.1 denotes the CP length of the first OFDM symbol.

Table 2.1: OFDM parameters in LTE downlink transmission

Channel bandwidth (MHz)	Max. number of occupied RBs	Occupied bandwidth (MHz)	FFT/ IFFT size	Number of occupied subcarriers	CP length (Samples)
1.4	6	1.08	128	6×12 = 72	9 (10)
3	15	2.7	256	15×12 = 180	18 (20)
5	25	4.5	512	25×12 = 300	36 (40)
10	50	9.0	1024	50×12 = 600	72 (80)
15	75	13.5	1536	75×12 = 900	108 (120)
20	100	18.0	2048	100×12 = 1200	144 (160)

The occupied bandwidth corresponds to the total number of active RBs in the downlink transmission, and it is equal to the number of active RBs multiplied by 180 kHz, where

180 kHz represents the frequency occupation of one RB. On the other hand, the channel bandwidth corresponds to the width of the channel.

2.5 Pilot distribution in LTE subframe

Pilots are used in the downlink transmission to enable the receiver to obtain the frequency response of the channel at certain time and frequency locations and facilitate the channel estimation and interpolation stage to get the channel responses for all the data subcarriers.

In LTE, the pilots are inserted in the first and the fifth OFDM symbols of each slot when using normal CP with six subcarriers spacing between pilots in the same OFDM symbol as shown in figure 2.4 [20].

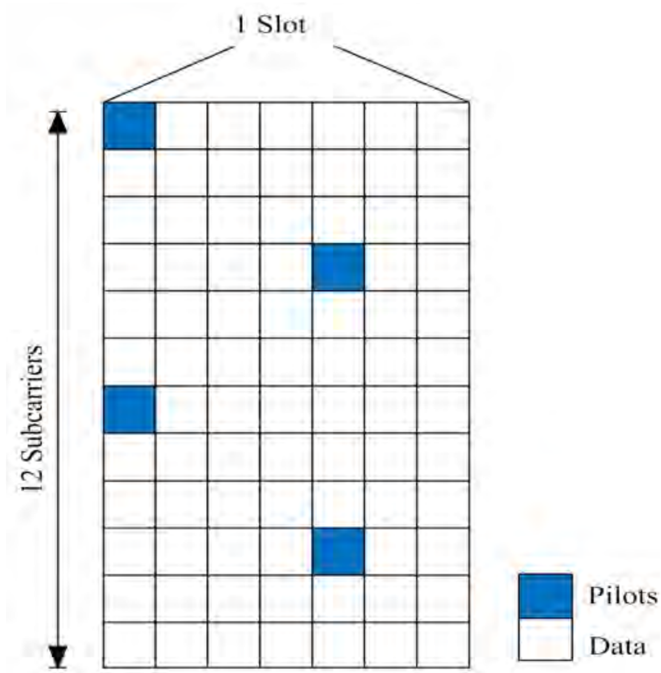

Figure 2.4: Pilot distribution in LTE downlink transmission slot

The frequency and time spacing between pilots are chosen such that they fulfill the Nyquist sampling theorem, which enables good channel estimation with relatively easy algorithms [22].

The minimum spacing in time domain (S_t) should be less that the channel variation in time domain, which is represented by the doppler spread (B_d), while the minimum spacing in frequency domain (S_f) has to be less than the inverse of the maximum delay spread (T_d^{max}) of the channel; this yields:

$$S_t < \frac{1}{B_d} \tag{2.1}$$

$$S_f < \frac{1}{T_d^{max}} \tag{2.2}$$

With such a pilot distribution, the ratio of pilot-to-information symbols is small which makes the full channel estimation a challenging problem but on the other hand maximizes the amount of transmitted information and allows for various algorithms to be developed to utilize this scattered distribution to keep tracking of the time variation across the OFDM symbols.

2.6 Turbo coding and decoding

Channel coding is used in most digital communication and especially in mobile communication to improve the error correcting capability. The LTE standards have adopted turbo coding.

The scheme of the turbo encoder shown in figure 2.5 is a parallel-concatenated convolutional code with two 8-state convolutional encoders and one internal turbo code interleaver and a bit reordering block to reorder the coded bits. The performance of the turbo encoder depends critically on the interleaver structure [15], where the turbo coding interleaver vector (X) in LTE is set as follows:

$$\mathrm{X(i)} = \mathrm{mod}(\mathrm{F_1\, i} + \mathrm{F_2\, i^2}, \mathrm{k}), \tag{2.3}$$

where $\mathrm{F_1}$ and $\mathrm{F_2}$ are chosen from the LTE specification depending on the frame size k and the modulation scheme used [15, 16].

The decoding of turbo codes is based on the A Posterior Probability (APP) algorithm iterative decoder. Two APP decoders are used in an iterative way, where the output from each decoder at a certain iteration acts as the priori probability for the other decoder.

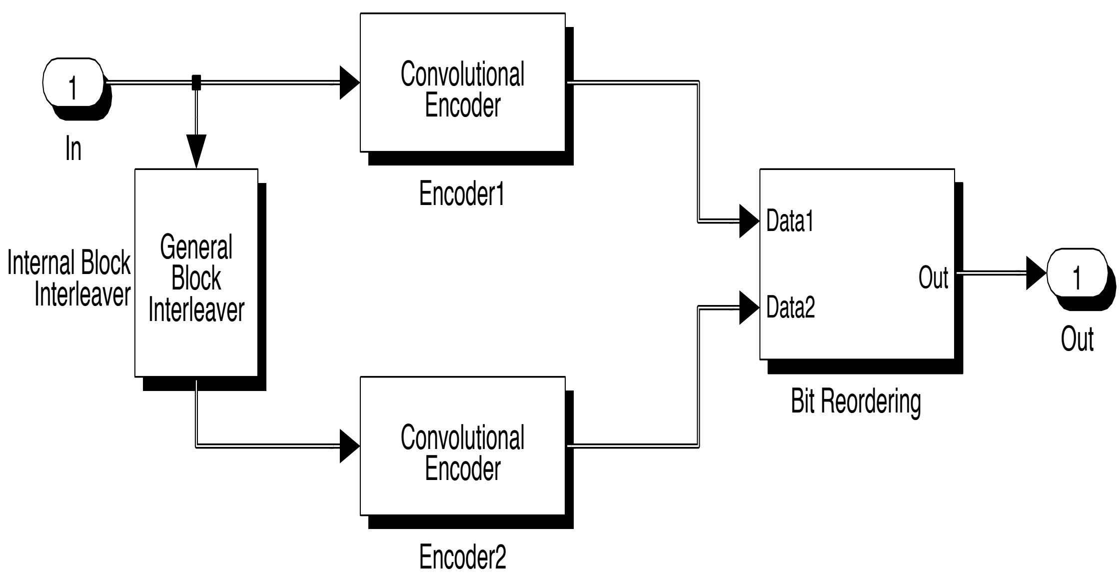

Figure 2.5: The turbo encoder structure in the LTE transmitter

Chapter 3

LTE downlink system model implementation

3.1 LTE-OFDM Simulink based model

The entire system evaluation is carried out on the Simulink platform, where the system consists of four main parts: transmission, reception, channel modelling and channel estimation.

The system is considered as a complex baseband model, which reduces the simulation time compared to a passband model. The Simulink model flowchart in figure 3.1 shows the proposed system model.

Most of the system components are built by using pre-defined Simulink blocks, which reduces the simulation time for the model. The OFDM modulator/demodulator, the interpolation block and the time-varying channel model are written using embedded MATLAB® function blocks.

The system is built as a frame-based system, with a frame size set according to the modulation and coding rate used, and a sampling frequency that corresponds to the frequency spacing between subcarriers and the IFFT/FFT size used.

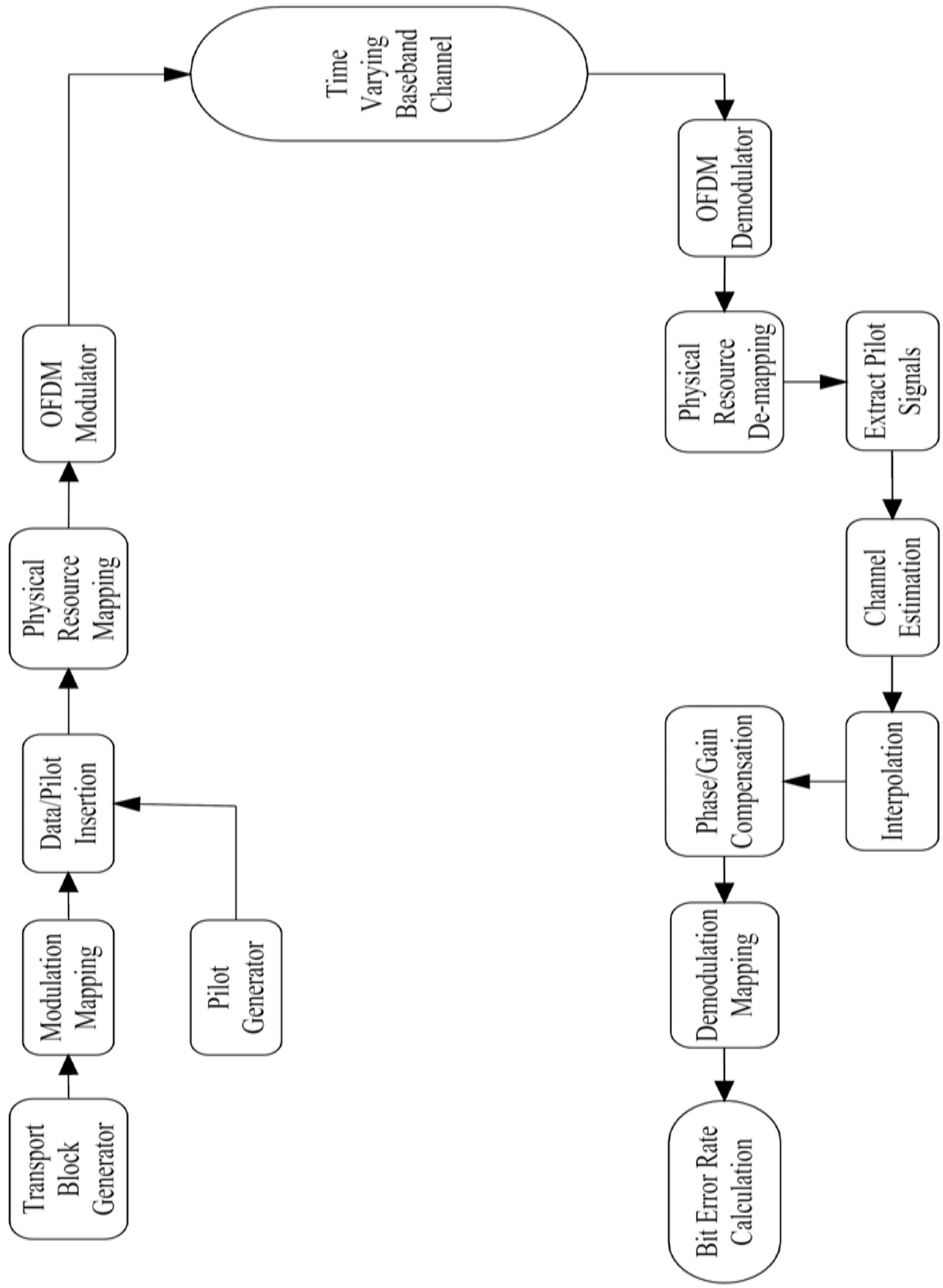

Figure 3.1: Simulink flow chart

3.2 Transmitter implementation

At the transmitter side, bits are randomly generated in a frame mode using the Bernoulli Binary Generator block, where the frame period is equal to the LTE slot period. The frame size is set according to the modulation and the coding rate indices in the LTE specifications for the 4-QAM and 1/3 coding rate. The information bits are then fed to the Turbo Coding block with the LTE-based interleaver mapping according to equation 2.3 that depends on the number of bits used in one transmission frame, where F_1 and F_2 are equal to 21 and 120, respectively, and k equals 320 bits per transmitted slot as shown in figure 3.2.

Due to the tail bit limits of each convolutional encoder in the turbo encoder, the encoder output code rate is slightly less than 1/3, which results in having an output of 972 coded bits frame. The Pad block is used to pad zeros at the end of the coded frame to set it to 960 bits per frame and fed the coded frame to the QAM modulator.

The coded bits are mapped then into complex modulated symbols according to the QAM scheme used. The Rectangular QAM Modulator block in Simulink is used for the modulation stage.

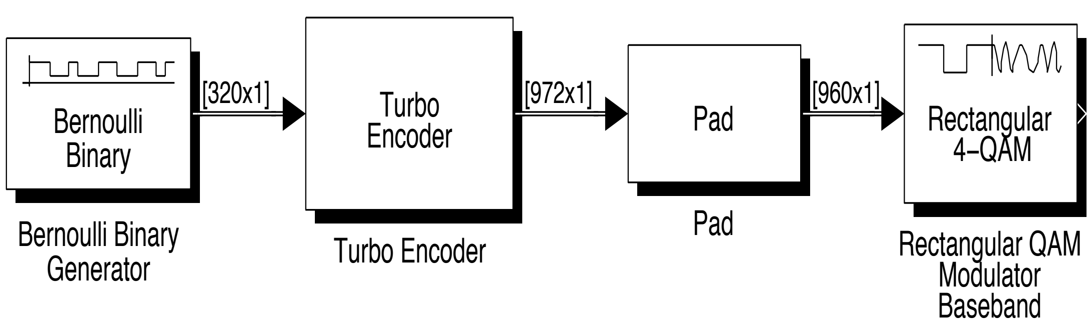

Figure 3.2: Coding and modulation of the data frame in Simulink

An embedded MATLAB function is written to insert the pilots among the modulated symbols according to the LTE specification. The output frame then is applied to a physical resource mapping stage as shown in figure 3.3.

At the physical resource mapping stage, the signal is re-shaped to match the LTE frequency-time domain grid that consists of seven symbols in the time domain and N subcarriers in the frequency domain for a normal CP length. In the LTE time-frequency grid, each column corresponds to one OFDM symbol and each row corresponds to one OFDM subcarrier.

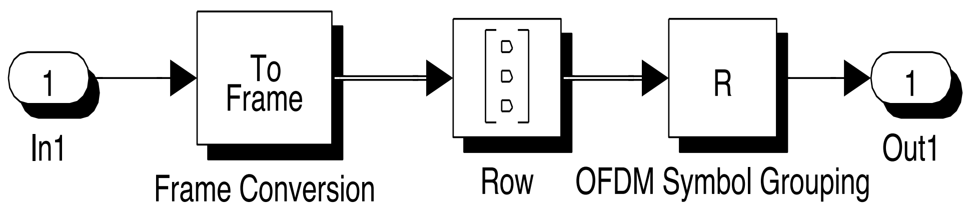

Figure 3.3: Physical resource mapping stage

The signal then is applied to the OFDM modulator as shown in figure 3.4, since not all the N subcarriers are used for data transmission; the unoccupied subcarriers are used as guard bands at the edges of the transmission frame.

In the OFDM modulator, the IFFT operation is applied across the N subcarriers to transform the modulated symbols to the time domain.

At the end, the time domain signal is extended by a CP, whose length is longer than the maximum delay spread. For example, the first OFDM symbol is extended by a CP length of ten samples and the remaining OFDM symbols are extended by a CP length of nine samples in the case of 128-point IFFT operation.

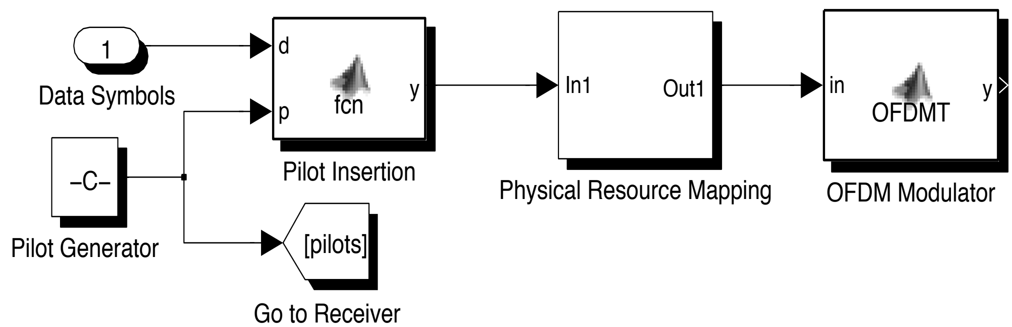

Figure 3.4: Pilot insertion, physical resource mapping and OFDM modulator in the Simulink model

3.3 Receiver implementation

The received signal $y(k)$ in discrete time can be expressed as follows:

$$y(k) = \sum_{l=0}^{L-1} h(k,l)\, d(k-l) + w(k), \tag{3.1}$$

where k is the discrete sampling time, L is the total number of channel paths, $h(k,l)$ is the impulse response of the time-varying channel and $w(k)$ is the additive white complex gaussian noise.

The transmitted signal $d(k)$ is given by:

$$d(k) = \frac{1}{\sqrt{N}} \sum_{n=0}^{N-1} s_n\, e^{\frac{j2\pi kn}{N}}, \tag{3.2}$$

where the sequence s_n is the modulated data symbols for n= 0,1... N -1.

At the receiver side, the CP is removed and an N-point FFT operation is applied to transform the signal back to the frequency domain.

By using equation 3.2 in equation 3.1, the received signal can be expressed as:

$$y(k) = \frac{1}{\sqrt{N}} \sum_{n=0}^{N-1} s_n \sum_{l=0}^{L-1} h(k,l)\, e^{\frac{j2\pi(k-l)n}{N}} + w(k) \tag{3.3}$$

The output of the OFDM demodulator after the N-point FFT operation at the nth subcarrier is given by:

$$Y_n = \frac{1}{\sqrt{N}} \sum_{k=0}^{N-1} y(k)\, e^{-\frac{j2\pi kn}{N}} = s_n H_n + I_n + W_n, \tag{3.4}$$

where n and k are the discrete frequency and time indices, respectively. H_n is the frequency domain channel response given by:

$$H_n = \frac{1}{N} \sum_{k=0}^{N-1} \sum_{l=0}^{L-1} h(k,l) e^{-\frac{j2\pi l n}{N}} \tag{3.5}$$

I_n represents the ICI caused by the time-varying channel and it is expressed as:

$$I_n = \frac{1}{N} \sum_{\substack{i=0 \\ i \neq n}}^{N-1} s(i) \sum_{k=0}^{N-1} H_i(k)\, e^{\frac{j2\pi k(i-n)}{N}} \tag{3.6}$$

W_n is the discrete fourier transform of the white gaussian noise, given as:

$$W_n = \frac{1}{\sqrt{N}} \sum_{k=0}^{N-1} w(k) e^{-\frac{j2\pi kn}{N}} \tag{3.7}$$

After the OFDM demodulator, the frequency domain signal is re-shaped in the physical resource de-mapping stage. After that the signal is passed to the channel estimation and interpolation stage as shown in figure 3.5.

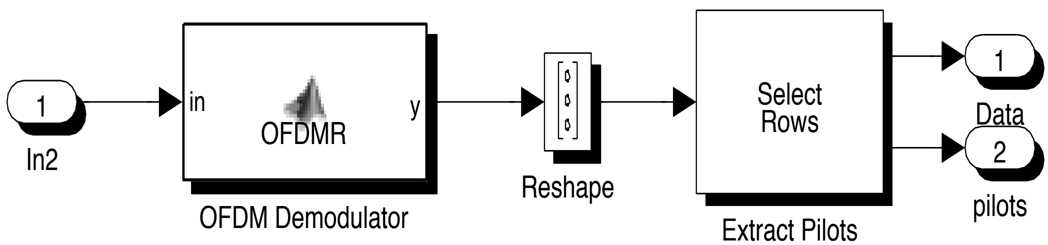

Figure 3.5: OFDM demodulator and pilot extraction implementation

At the channel estimation and interpolation stage, first, the pilots are extracted from the data subcarriers using the Multiport Selector block - which is renamed here as the Extract Pilots block in figure 3.5- and the channel frequency response is obtained at the pilot tones using the LS channel estimation method as follows:

$$H_n = \frac{Y_n}{P_n}, \tag{3.8}$$

where H_n is the channel frequency response at the pilot n, Y_n is the received pilot signal and P_n denotes the transmitted pilot signal [28].

The obtained channel frequency responses at the pilot symbols are fed to an embedded MATLAB function to employ the interpolation stage in both time and frequency domains as shown in figure 3.6.

Once the full channel response is obtained from the interpolation stage, a gain and phase compensation stage is applied among the information symbols to compensate for any gain loss and/or phase shift resulting from the time-varying channel.

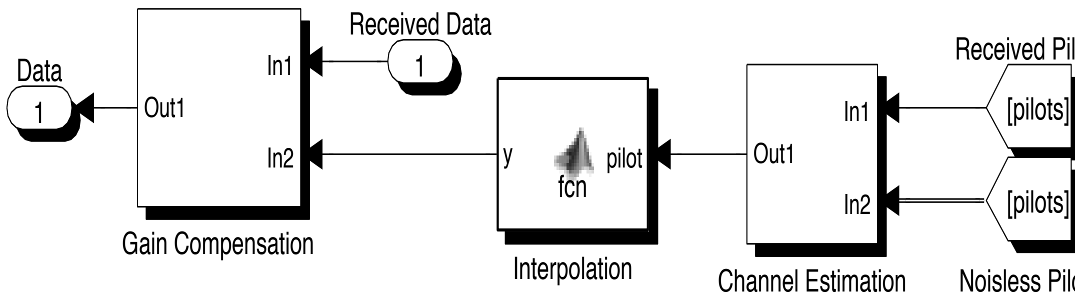

Figure 3.6: Channel estimation and interpolation stage implementation

The decoded information symbols are applied to a QAM demodulator implemented by the Rectangular QAM Demodulator block. The output recovered bits then are applied to a Pad block to remove the padded bits at the transmitter.

A Turbo Decoding block with a true APP decoding algorithm and six decoding iterations is used after; the same interleaver used in the Turbo Coding block is used in the decoding stage.

Before the BER calculations stage, delays and matching transmitted and received frame sizes have to be carefully considered for accurate results.

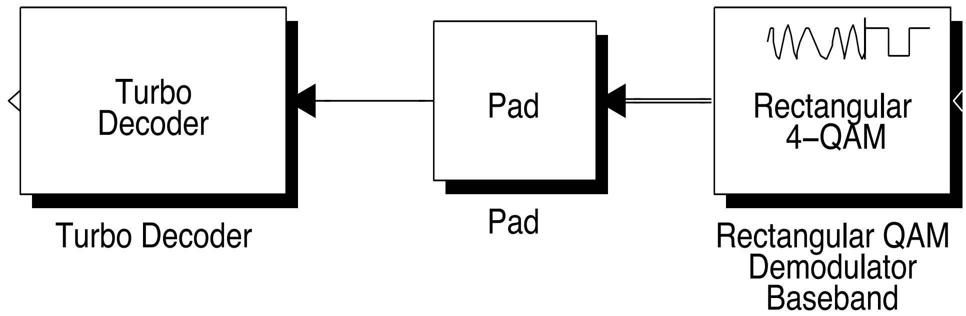

Figure 3.7: QAM demodulation and turbo decoding in Simulink

The BER calculations are carried out using the Error Rate Calculation block at the end of the model to evaluate the performance of the system.

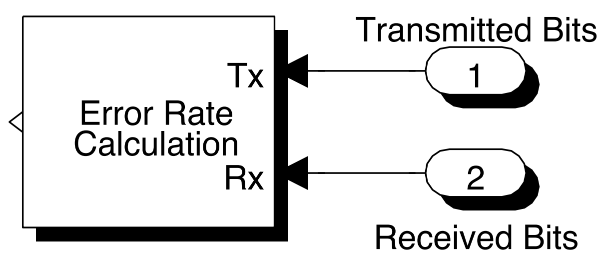

Figure 3.8: BER calculation implementation

3.4 LTE channel models

The time domain signal is transmitted over a complex baseband time-varying channel, where the path delays and the path gains are set using the LTE channel models for different scenarios and velocities.

These models are: the Extended Pedestrian A (EPA) model, the Extended Vehicular A (EVA) model and the Extended Typical Urban (ETU) model [17].

Figure 3.9 shows the Simulink implementation used for the channel models, where different doppler frequencies can be used for different mobile velocities.

The doppler frequencies used are 5 Hz for the EPA model, 70 Hz for the EVA model and 300 Hz for the ETU channel model.

Maximum delays of 410 ns, 2510 ns and 5000 ns for the LTE channel models as shown in table 3.1, which are well within the LTE specified long CP length of 16.67 μs.

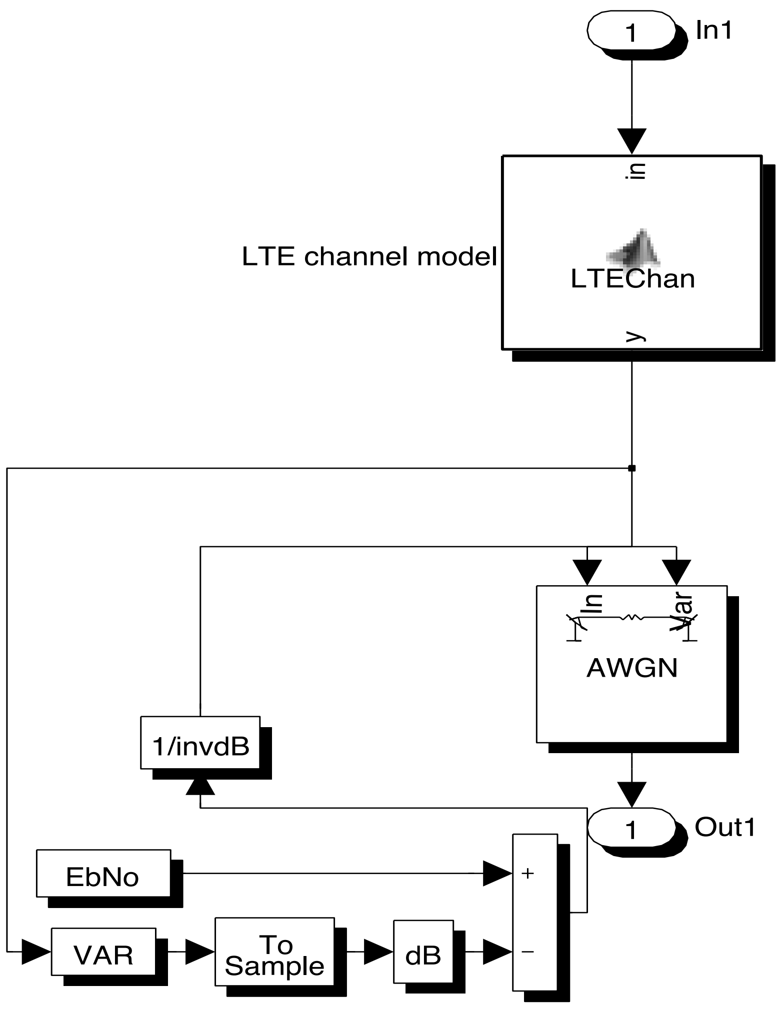

Figure 3.9: Channel model implementation in Simulink

The EVA and ETU models have nine multipath components each, whereas the EPA model has seven multipath components as shown in table 3.1. The EPA model has a Root Mean Square (RMS) delay spread of 45 ns, while the EVA and the ETU models have an RMS delay spread of 357 ns and 991 ns, respectively.

Table 3.1: The multipath profile of the LTE channel models

	Extended Pedestrian A model (EPA)		Extended Vehicular A model (EVA)		Extended Typical Urban model (ETU)	
Tap	Tap delay (ns)	Relative gain (dB)	Tap delay (ns)	Relative gain (dB)	Tap delay (ns)	Relative gain (dB)
1	0	0	0	0	0	-1
2	30	-1	30	-1.5	50	-1
3	70	-2	150	-1.4	120	-1
4	90	-3	310	-3.6	200	0
5	110	-8	370	-0.6	230	0
6	190	-17.2	710	-9.1	500	0
7	410	-20.8	1090	-7	1600	-3
8	-	-	1730	-12	2300	-5
9	-	-	2510	-16.9	5000	-7

Chapter 4

Channel estimation and interpolation in LTE-OFDM based systems

4.1 Introduction

In OFDM-based systems, different algorithms, which vary in computational complexity and accuracy, can be used for the channel estimation stage. Since LTE-based systems use coherent detection of the transmitted data, an estimate of the channel response has to be available at the receiver. Thus, the need arises to develop a reliable channel estimator and interpolator for data detection.

The Least Square (LS) and Minimum Mean Square Error (MMSE) criteria are common methods to estimate the channel coefficients. A brief explanation about these estimators is provided in the following sections. The BEM is also briefly investigated too given its wide use in general OFDM-based systems in tracking the time variation of the channel.

More detailed analysis for the 2D linear interpolation and the proposed algorithm are provided later in this chapter.

4.2 Pilot-assisted channel estimation

In a high-mobility environment, pilot symbols play a significant role in tracking the channel variation over time, if they are appropriately placed over time and frequency.

The pilot distribution over the transmission frame in OFDM-based systems has many types, called block, comb and scattered, which is the one that is adopted in the LTE standard.

In pilot-assisted channel estimation, the initial channel estimation at the pilot tones is first obtained using one of the common channel estimation methods such as the LS and MMSE methods and then an interpolation technique is applied over the OFDM symbols in both time and frequency domains to obtain the channel frequency responses for the data subcarriers.

Due to the scattered distribution of pilots in the LTE downlink transmission frame, performing channel estimation and interpolation might be challenging depending on the approach used [28]. To overcome this challenge, we need to develop more complex linear interpolation techniques, where the channel response for each data subcarrier can depend more on the received pilot tones and take advantage of this scattered distribution.

4.2.1 The LS method

The frequency domain of the LS-estimated channel frequency response ($\hat{h}_p$) at the received pilot tones (y_p), with the noiseless transmitted pilot symbols (x_p), can be obtained as [23, 25]:

$$\hat{h}_p = x_p^{-1}\, y_p \tag{4.1}$$

$$\hat{h}_p = \left[\frac{y_p(0)}{x_p(0)}\,\frac{y_p(1)}{x_p(1)} \cdots \frac{y_p(N_p-1)}{x_p(N_p-1)}\right] \tag{4.2}$$

N_p denotes the total number of pilots used in the channel estimation and $\hat{h}_p$ is a vector of size $N_p \times 1$. The LS does not use the two-dimensional statistics of the channel, which makes it a low complexity estimator, but on the other hand it results in a high mean square error.

4.2.2 The MMSE method

The MMSE estimated channel frequency response $\hat{h}$ assuming all pilots have the same transmitted power can be expressed as:

$$\hat{h} = R_{h\hat{p}} R_{\hat{p}\hat{p}}^{-1} y_{\hat{p}} \tag{4.3}$$

$$R_{h\hat{p}} = E\{ h\hat{p}^H \} \tag{4.4}$$

$$R_{\hat{p}\hat{p}} = E\{ \hat{p}\hat{p}^H \} = R_{pp} + \frac{1}{SNR} I, \tag{4.5}$$

where $R_{h\hat{p}}$ is the cross-covariance matrix of size $N_h \times N_p$ between h and the received pilots $\hat{p}$, where N_h corresponds to the total number of channel estimates for the subcarriers. $R_{\hat{p}\hat{p}}$ is the auto-covariance matrix of the pilot estimates of size $N_p \times N_p$, $y_{\hat{p}}$ is the received pilot tones with size of $N_p \times 1$, R_{pp} is the auto-covariance matrix of the transmitted noiseless pilots with a size of $N_p \times N_p$, $E\{ x \}$ represents the mathematical expectation of the variable x and I is the identity matrix with size of $N_p \times N_p$.

The MMSE estimator suffers from a high computational complexity compared to the LS estimator but gives better mean square error performance. Another drawback of the MMSE estimator is the assumption of the knowledge of two-dimensional statistics of the channel at the receiver, which is not available all the time [3, 23].

4.2.3 Basis Expansion Model

BEM is explored due to its estimation accuracy and the reduction of the number of parameters that need to be estimated in fast time-varying channels [10].

The channel in BEM is expressed as a superposition of known basis functions weighted by unknown time-invariant basis coefficients approximating the variation of the channel during a specific window time [11]; thus the channel estimation problem is converted to the estimation of a limited number of basis coefficients [12, 13].

The number of basis functions depends on the doppler frequency and the length of the time window used; thus the BEM assumes knowledge of the maximum doppler frequency at the receiver.

BEM has higher computational complexity than 2D linear models [10], and increasing the mobile velocity degrades its performance significantly, since the sensitivity of the BEM estimator to the estimation error increases in consequence.

The BEM channel estimation steps can be essentially summarized in the following points:

1. Find the BEM time-invariant coefficients by using either the LS or MMSE methods.
2. Find the channel impulse response with a factor that is used as a tradeoff between complexity and the needed accuracy.
3. Calculate the number of basis functions to be used based on the knowledge of the maximum doppler frequency.

4.3 2D linear interpolation method

The Piecewise Linear (PWL) model is investigated since it is considered one of the simplest estimators [8] that requires a minimum number of operations and still shows sufficient estimation accuracy for speeds up to 120 km/hr in some OFDM systems [2]. Based on its features, this model promises with some modifications a sufficient estimation accuracy that can be obtained in LTE-based systems for fast time-varying channels [9].

Two consecutive pilots are required to determine the channel response for data subcarriers between them in the PWL model. The channel response $\mathrm{H}(\mathrm{F_d})$ for data subcarrier $\mathrm{F_d}$ between pilot subcarriers $\mathrm{F_p}$ and $\mathrm{F_{p+1}}$ can be expressed as [26]:

$$\mathrm{H}(\mathrm{F_d}) = \left(\frac{\mathrm{H}(\mathrm{F_{p+1}}) - \mathrm{H}(\mathrm{F_p})}{\mathrm{F_{p+1}} - \mathrm{F_p}}\right)(\mathrm{F_d} - \mathrm{F_p}) + \mathrm{H}(\mathrm{F_p}) \tag{4.6}$$

and an extrapolation method is applied for the data subcarriers outside the pilots range in the same OFDM symbol. This can be expressed as:

$$\mathrm{H}(\mathrm{F_d}) = \left(\frac{\mathrm{H}(\mathrm{F_p}) - \mathrm{H}(\mathrm{F_{p-1}})}{\mathrm{F_p} - \mathrm{F_{p-1}}}\right)(\mathrm{F_d} - \mathrm{F_p}) + \mathrm{H}(\mathrm{F_p}) \tag{4.7}$$

The channel frequency response is first obtained at the pilot tones, and then the linear interpolation is applied in the frequency and the time domain to obtain the channel response of the data subcarriers as shown in figure 4.1.

In the conventional 2D linear interpolation method, it can be noticed that the channel estimates of the data subcarriers do not depend directly on the pilot's channel estimates for most of the OFDM symbols.

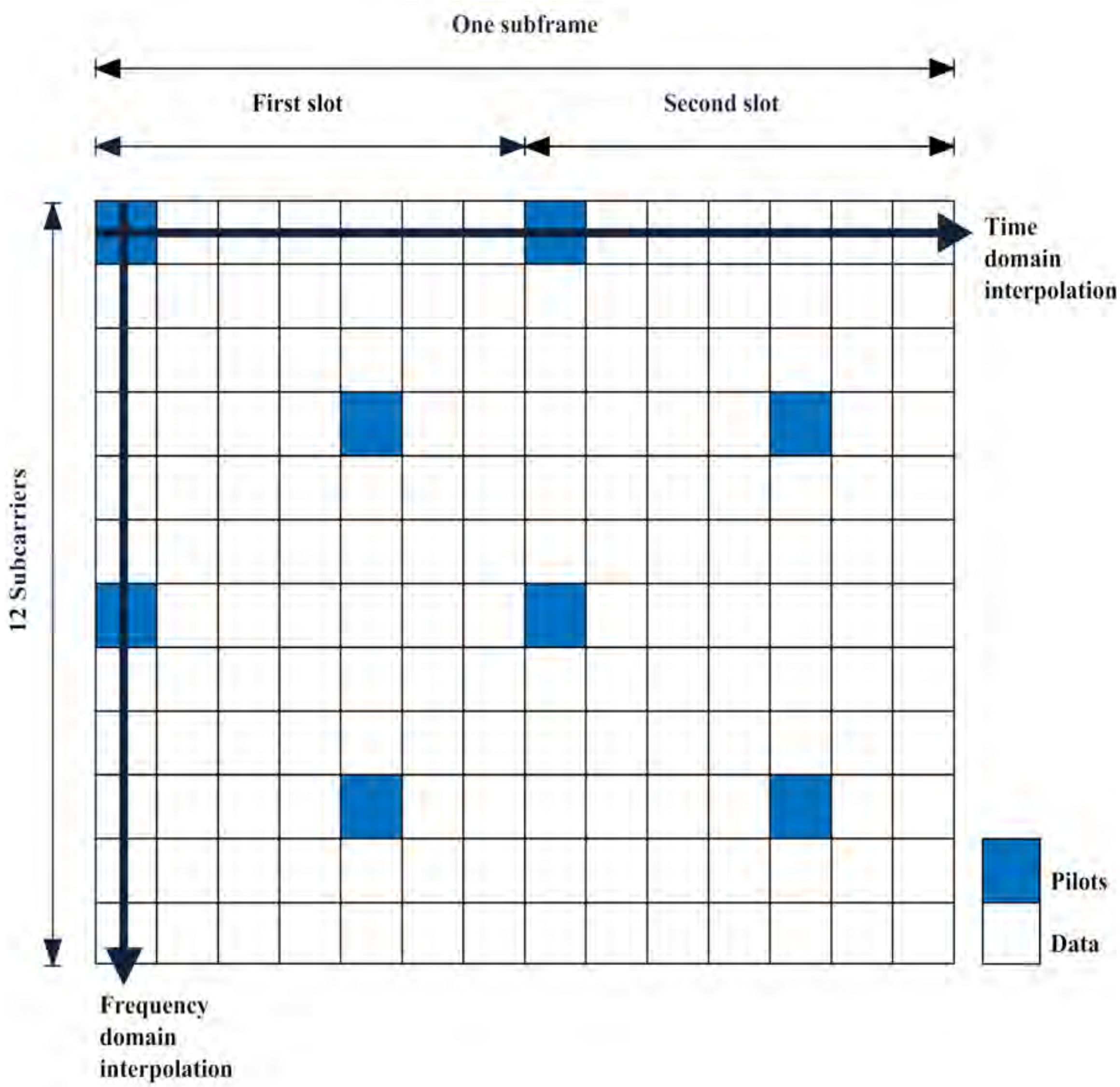

Figure 4.1: Two-dimensional linear interpolation over one subframe

To clarify more, the data subcarriers of the first and the fifth OFDM symbols depend on their channel estimates of the two nearest pilots, where the data subcarriers of the remaining OFDM symbols depend on the interpolated channel estimates of the first and the fifth OFDM symbols, which are not necessarily accurate. Such a method results in a poor estimate in fast time-varying channels.

4.4 Modified 2D linear interpolation method

In a high-mobility environment, the time variation is unlikely to be a simple linear function. Studying the time and frequency correlation relations in LTE-OFDM based systems, we incorporate both linear interpolation and time-frequency correlation characteristics of the channel to improve the obtained channel estimates while maintaining a low-complexity level in terms of the needed processing time.

4.4.1 Time and frequency correlation functions

The OFDM time and frequency correlation functions are used in the proposed method, where the use of fixed pilot positions in every slot can be utilized to explore the channel characteristics in time and frequency domain at the receiver [22].

For a multipath power delay profile, the correlation function in frequency is given by:

$$R_f(n) = \frac{1}{1 + j2\pi\, T_{rms}\, n\, \Delta f}, \tag{4.8}$$

where Δf is the subcarrier spacing of 15 kHz, n is the subcarrier number, and T_{rms} is the Root Mean Square (RMS) time of the channel [27].

For a time-varying signal with maximum doppler frequency F_d^{max} and a Jakes' doppler spectrum as in figure 4.2, the correlation function in time is expressed as [21, 24]:

$$R_t(l) = J_0(2\pi\, F_d^{max}\, l\, T_s), \tag{4.9}$$

where $J_0(x)$ is the zeroth-order Bessel function of the first kind, l represents the OFDM symbol number and T_s is the OFDM symbol duration.

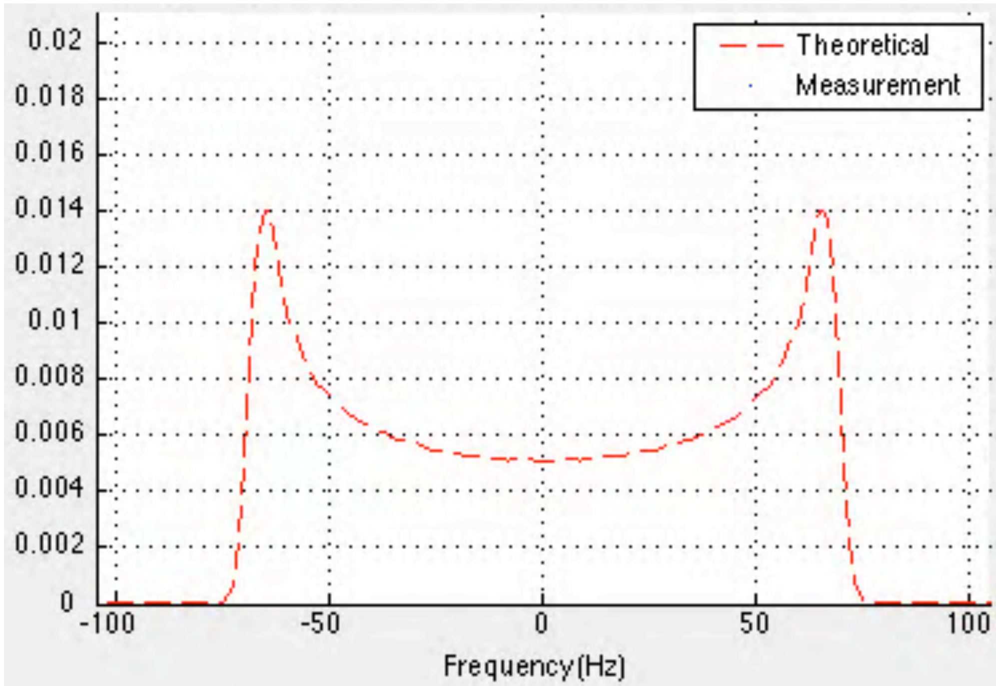

Figure 4.2: Jakes' doppler spectrum for 70 Hz

The assumptions behind the used time correlation function are:

1. horizontal radio wave propagation,
2. the angle of arrival of the radio waves at the mobile is uniformly distributed over $[0, \pi]$,
3. the power arrives uniformly from all angles for all velocities and
4. the antenna used at the receiver is omnidirectional.

4.4.2 Methodology

The idea of the proposed method is to improve channel estimates for each subcarrier by identifying more dependencies among channel estimates and utilizing the channel characteristics to improve the obtained estimates. This in consequence should improve the channel estimates of these data subcarriers and improve the overall system performance.

It was found from different simulation tests that the marked data subcarriers in figure 4.3 tend to have poor channel estimates since they do not depend directly in their channel estimates on the pilot estimates. Because of that, the proposed method tries to improve the channel estimates of these data subcarriers and make them more reliable.

Although channel estimates of the OFDM symbols at the edge of a slot also tend to be inaccurate, this can be improved by using the channel estimates from a previous slot. A more detailed explanation for this method is provided later.

First, a full channel-estimate matrix is obtained using a conventional 2D linear interpolation method; the frequency channel response along the frequency domain is obtained at the pilot tones using the LS method, then linear interpolation is applied in the frequency domain direction between the pilot subcarriers to obtain the channel estimates for all the data subcarriers in the first and the fifth OFDM symbols.

These data subcarriers can be considered as secondary pilots, where they are used to track the channel time variation of all subcarriers over the adjacent OFDM symbols.

Subsequent linear interpolation in the time domain direction is applied between the first and the fifth OFDM symbols to obtain the channel estimates for all the data symbols between them and a linear extrapolation method is applied at the fifth OFDM symbol to obtain the channel estimates for the last two OFDM symbols in a slot.

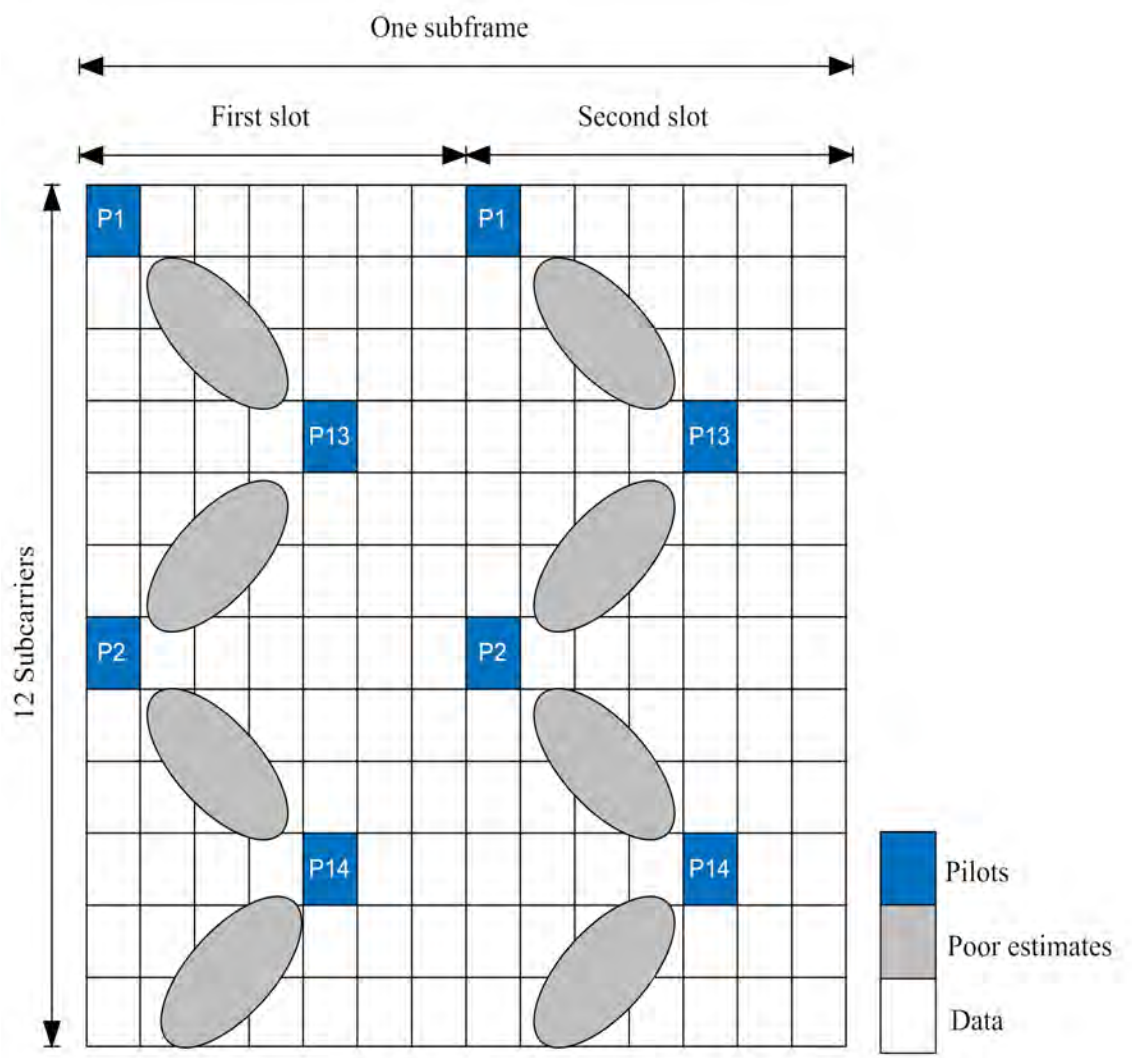

Figure 4.3: Targeted resource elements in the proposed interpolation method

Once the full channel estimation matrix is obtained, the time and frequency correlation relationships in equations (4.8) and (4.9), are solved to get the correlation values for the marked data subcarriers in figure 4.3 between the pilots of the first to the fifth OFDM symbols, over the time and frequency, where the correlation values are evaluated for the resource elements between (P1) and (P13) and then between (P13) and (P2) and so on until the last two pilots in all of the OFDM symbols in one slot. Pilot (P1) is the starting point for the channel evaluations over time and frequency.

The time correlation function is solved starting from one pilot at the first OFDM symbol to the next pilot at the fifth OFDM symbol or the other way around, and it is solved for l = T, 2T and 3T, where T denotes the total OFDM symbol time, which equals the effective symbol length and the CP length. The maximum time (3T) is equal to the maximum time between the pilots from the first or the fifth OFDM symbol and the data subcarriers in between. The frequency correlation function is solved for n = Δf, 2Δf and 3Δf, where 3Δf represents the maximum frequency spacing between (P1) and (P13), and between (P13) and (P2) and so on.

By exploring the Jakes' correlation model among the OFDM symbols in time and frequency domains between every two pilot symbol pairs, more channel estimation dependencies are obtained, which enhances the capability of the channel estimator and interpolator to improve the channel estimates for the data subcarriers at these OFDM symbols.

The channel estimates of the data subcarriers in the second, third and fourth OFDM symbols are then modified with the new obtained estimates by the time and frequency correlation relations to improve the obtained channel estimate at these resource elements.

This simple yet efficient method gives better channel estimates for the data subcarriers and improves the BER performance as shown in chapter 5.

A key point to notice is that the time and frequency correlation functions can be pre-solved for the targeted subcarriers since they do not depend on the received symbols; they depend on the position of the pilots in one slot and the number of pilots used in the downlink transmission.

This significantly reduces the computational complexity and the processing time of the estimator, since the correlation values for different doppler frequencies and RMS delay spread values can be pre-calculated and fed to the interpolator to be used depending on which channel the mobile is under.

To overcome the need to make the assumption of the knowledge of the doppler frequency and the RMS delay spread of the channel, the proposed method is tested for pre-calculated time-and-frequency correlation values under different LTE channel models that do not match the Doppler frequency used for the correlation calculations.

The Bessel function that describes the time correlation of the Jakes' doppler spectrum is evaluated for doppler frequencies at 70 Hz and 300 Hz for a time interval of three OFDM symbols, that is the number of OFDM symbols targeted between the first and the fifth symbols.

Figure 4.4 shows how close the two functions at different doppler frequencies are.

These results demonstrate the proposed method's reliability, since there is no need to make any assumption regarding the pre-knowledge of the doppler frequency at the receiver. These results also present a robust estimator, that is, an estimator that is not sensitive to the channel statistics such as the mobile velocity, since the channel statistics, which depend on the particular environment, are usually unknown at the receiver.

A fixed doppler frequency can be used at the interpolator that corresponds to the expected channel without affecting the BER performance significantly if the channel variation changed at some point.

As stated before, the channel estimates of the OFDM symbols at the edge of a slot or a transmission frame in general are poor. To solve this problem, interpolation over one subframe is performed with the addition of time and frequency correlation relations between the two slots in the subframe.

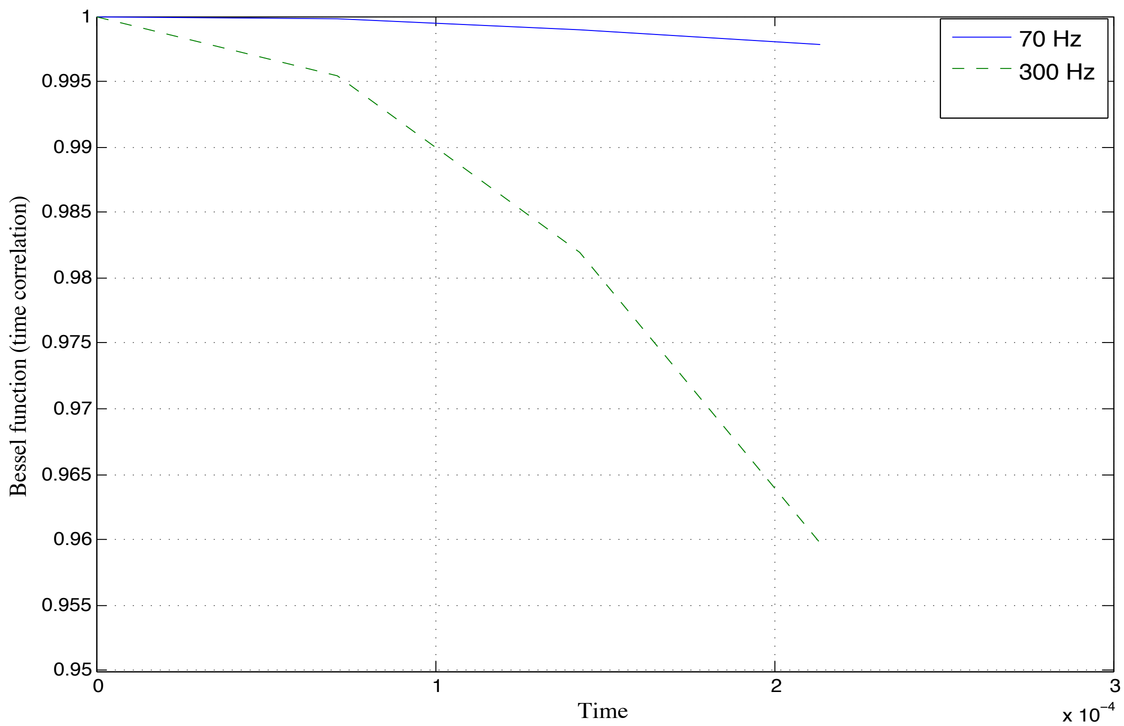

Figure 4.4: Time correlation relationships for 70 Hz and 300 Hz

The same methodology explained earlier for the one slot modified interpolation is used separately for the two slots in one subframe, and then the time and frequency correlation functions are solved to get the correlation values for the marked data subcarriers between the pilots of the fifth OFDM symbol and the eighth OFDM symbol as shown in figure 4.5.

The use of the previous slot's correlation values improves to some extent the obtained channel estimates at the edges of that slot, but introduces a delay due to the need to store each slot to be used by the next slot in a subframe.

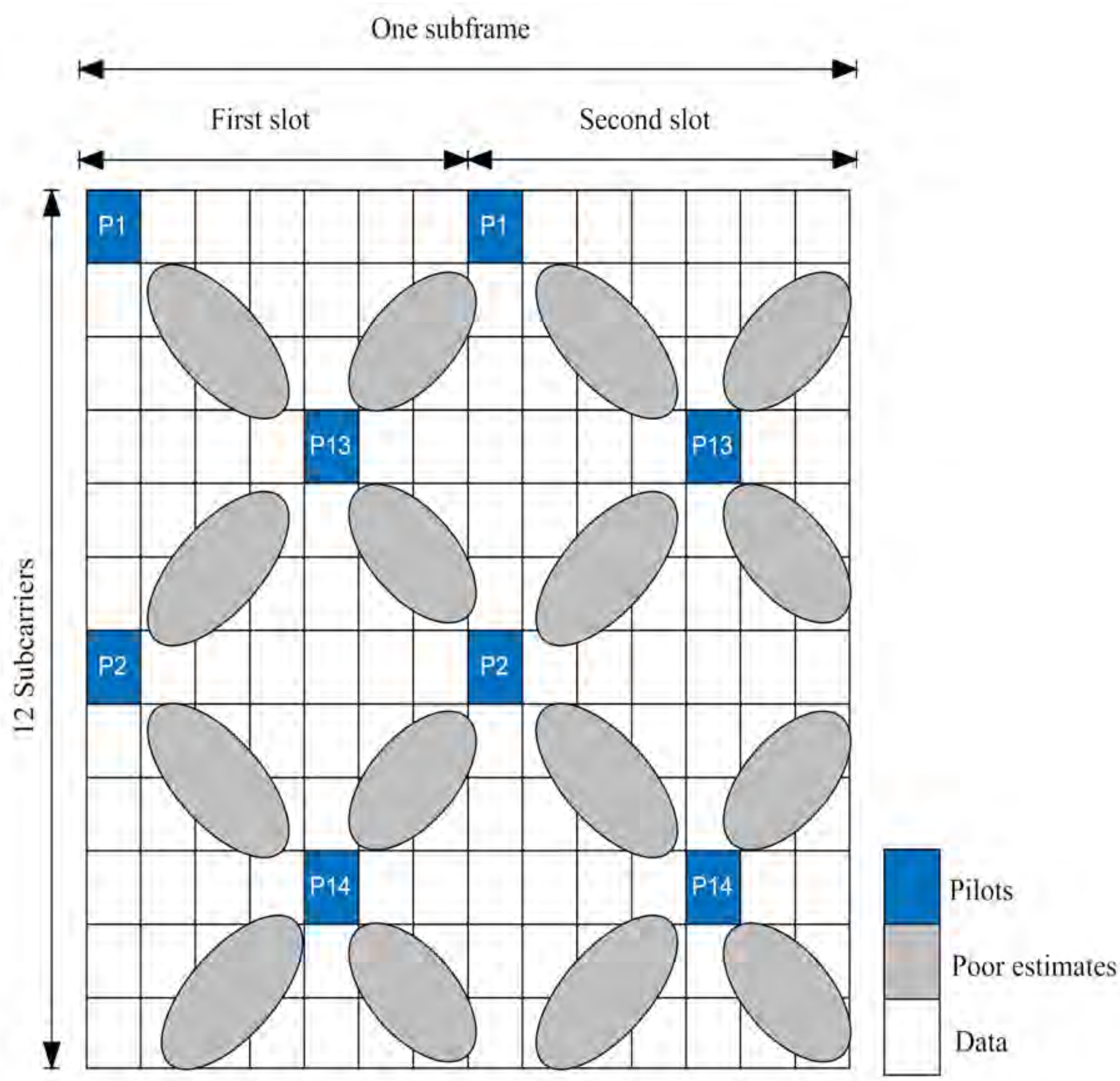

Figure 4.5: The modified interpolation method over one subframe

Chapter 5

Simulation and results

5.1 Simulation setup

As stated earlier, the platform that is used to build the downlink LTE-based system is Simulink. The LTE channel models described in chapter three have been tested for the proposed 2D linear interpolation and the conventional 2D linear interpolation methods, and the comparison is evaluated in terms of the BER performance and the required processing time. Table 5.1 details the simulation parameters used in the various tests.

The first part of the test is to evaluate the BER performance of the proposed method compared to the conventional method with the assumption of the knowledge of the doppler frequency at the receiver.

The second part is to test the proposed technique without any knowledge of the channel – fixed time and frequency correlation values – to see how robust the modified method is to any change in the mobile velocity.

Furthermore, the proposed solution to improve the channel estimates at the edges by performing the interpolation over one subframe is tested and compared to the interpolation over one slot.

The simulation is carried out on an Intel Core i5 processor with a 2.5 GHz clock speed.

The computational complexity of the system is measured in terms of the required processing time measured in seconds on the computer that is performing the simulations.

Table 5.1: Simulation parameters

Channel bandwidth	1.4 MHz
FFT/IFFT size	128 subcarriers
Number of pilots	48 pilots/slot
Number of OFDM symbols/slot	7 OFDM symbols
CP length	Normal
Transmitted frame size/length	1 slot = 0.5 ms 1 subframe = 1 ms
Sampling frequency (f_s)	1.92 MHz
Achievable data rate/subframe	2.016 Mbps
Modulation scheme	4-QAM
Number of bits/frame	320 bits
Transmitter × Receiver antennas	1 × 1

The achievable data rate for the above parameters is calculated for the 4-QAM modulation scheme as:

$$\text{Data rate} = \frac{12\ \text{subcarriers} \times 7\ \text{OFDM symbols} \times 6\ \text{RBs} \times 2\ \text{slots} \times 2\ \text{symbols}}{1\ \text{ms}} \tag{5.1}$$

and the sampling frequency $\mathrm{f_s}$ used is computed as follows:

$$\mathrm{f_s} = \mathrm{N}\ \Delta\mathrm{f} \tag{5.2}$$

5.2 BER performance with the knowledge of the doppler frequency

The BER performance is evaluated for the modified and the conventional 2D interpolation methods assuming the knowledge of the doppler frequency at the receiver.

The proposed method uses only the correlation values computed for the 70 Hz or 300 Hz doppler frequencies, since they represent fast time-varying channels.

Figures 5.1, 5.2 and 5.3 show the BER performance results for the three channel models compared to the BER performance of QAM over the Additive White Gaussian Noise (AWGN) channel with no motion.

For the EPA 5Hz channel model, the correlation values for the 70 Hz Jakes' spectrum are used, since the time variation in the EPA 5Hz is not significant and the Bessel function of Jakes' relationship gives close values for both of the doppler frequencies.

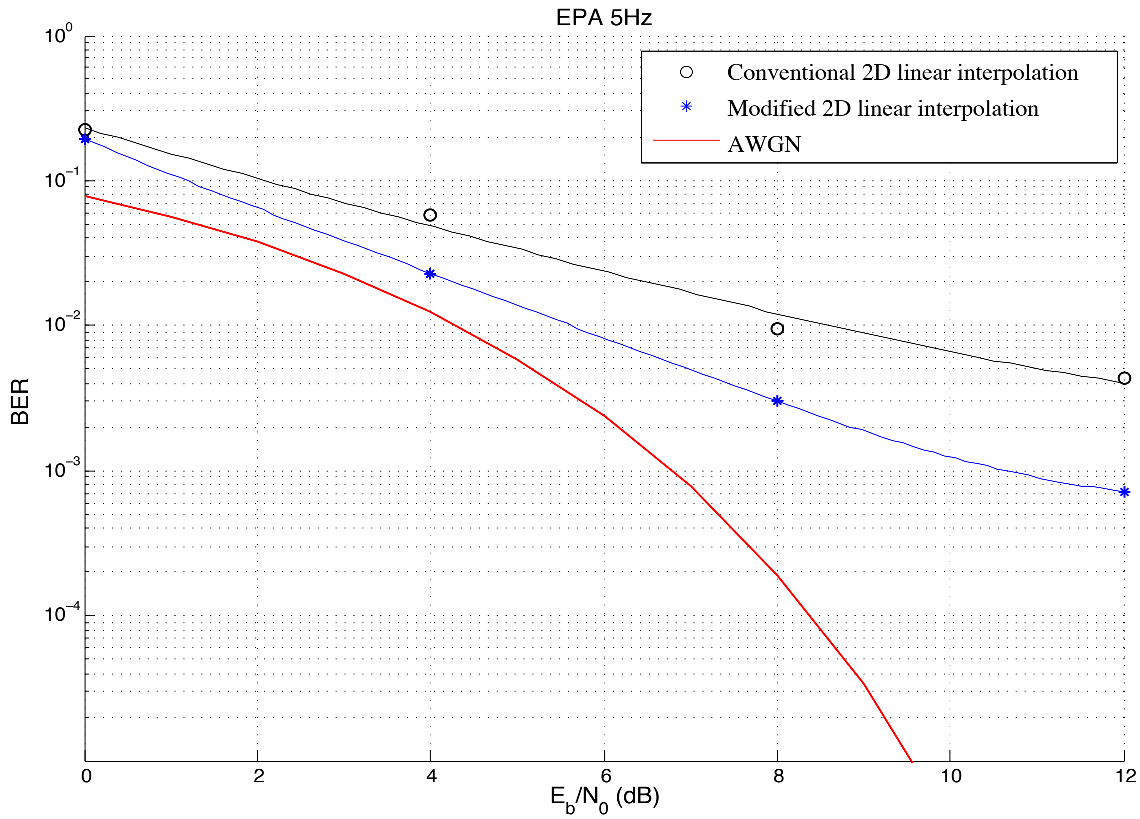

Figure 5.1: BER performance under the EPA 5Hz channel model

At E_b/N_0 = 12 dB, BERs of 0.06%, 0.6% and 2% are obtained from the proposed method for EPA 5Hz, EVA 70Hz and ETU 300Hz channel models, respectively. In contrast, the conventional method gives BERs of 0.4%, 2.5% and 6% for EPA 5Hz, EVA 70Hz and ETU 300Hz, respectively.

It can be noticed from the results, the significant improvement of the BER performance obtained from the proposed method.

This improvement comes from the advantage of exploring the time and frequency characteristics of the Jakes' doppler spectrum over the LTE transmission grid, and the new use of the LTE pilot distributed channel estimates to improve the obtained channel estimates at the data subcarriers.

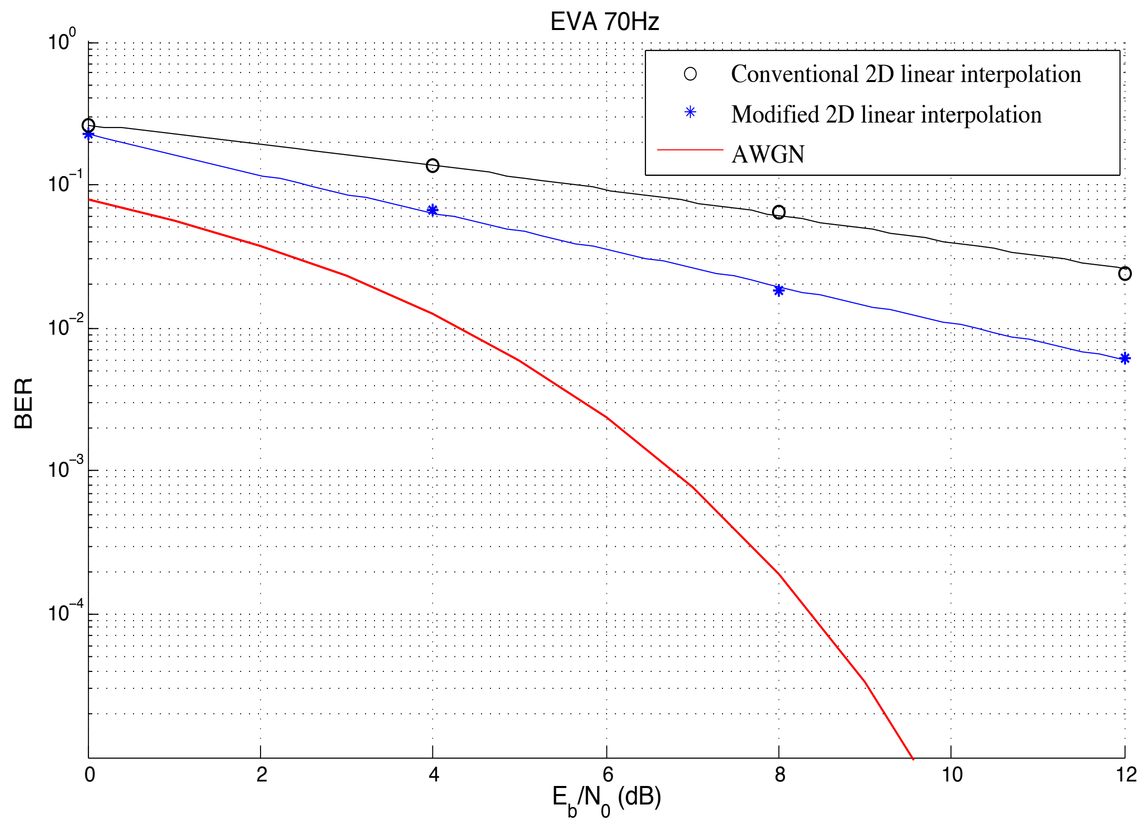

Figure 5.2: BER performance under the EVA 70Hz channel model

For the EPA 5Hz and the EVA 70Hz channel models, the correlation values of the 70 Hz Jakes' spectrum are used, while the 300 Hz Jakes' spectrum correlation values are used for the ETU 300Hz channel model.

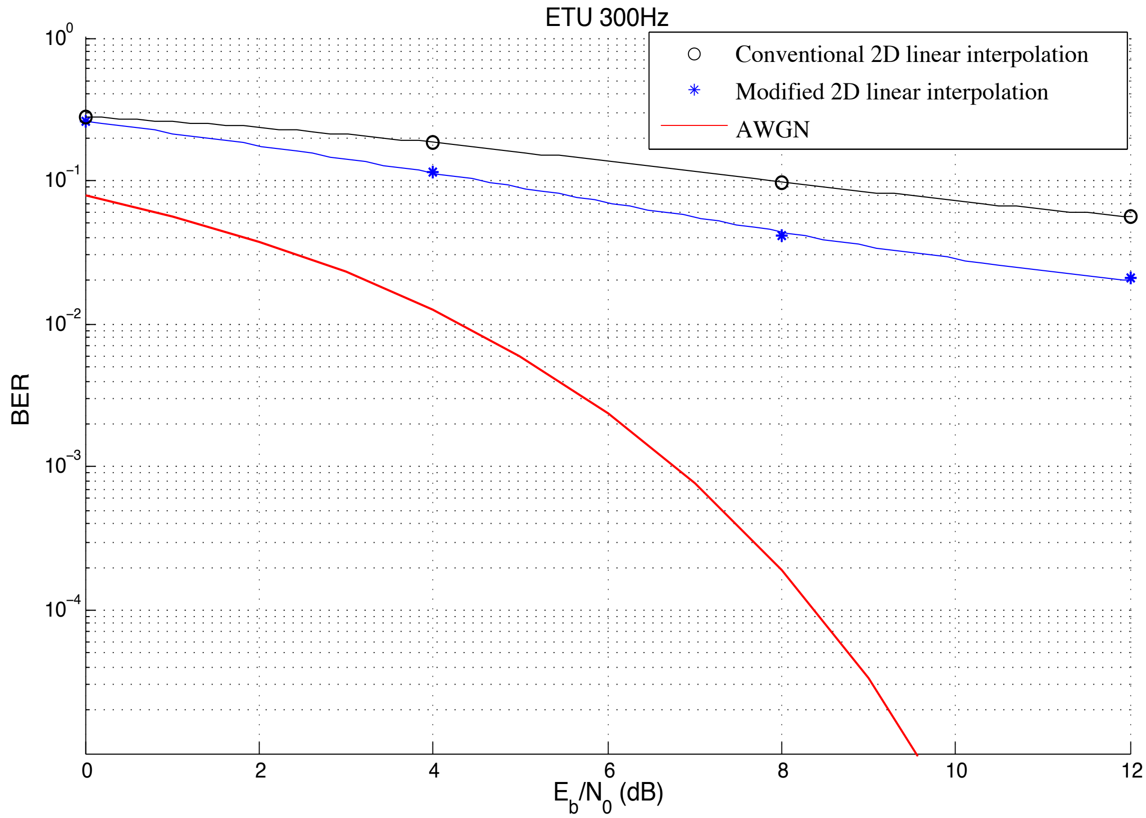

Figure 5.3: BER performance under the ETU 300Hz channel model

Table 5.2 shows the required processing time of the proposed method compared to the conventional one at E_b/N_0 = 8 dB. As it can be noticed, the time per call for the conventional 2D linear interpolation method is approximately the same for the three channel models, since it does not depend on the mobile speed or the channel multipath profile.

The time per call stands for the time required by the computer used in the simulation tests to perform interpolation over all data subcarriers for each slot.

The processing time per call increases when the proposed method is used, where an increase of 42.8% is required when using the modified method for the 70 Hz correlation values with the EPA 5Hz channel, 37.6% increased processing time is needed when using it for the EVA 70Hz channel and for the ETU 300Hz channel, an increase of 33.2% in the required processing time is needed for the proposed method.

The increase in the required processing time for the proposed method is not significant, since the linear interpolation is a low-complex method and requires a low processing time, such features make the 42.8% increase in the processing time not considered as a high increase.

Table 5.2: Processing time comparison between the proposed methods and the conventional 2D method

	EPA 5Hz channel		EVA 70Hz channel		ETU 300Hz channel	
Method	Time percentage (%)	Time/call (ms)	Time percentage (%)	Time/call (ms)	Time percentage (%)	Time/call (ms)
Conventional 2D	0.950	0.223	1.10	0.255	1.10	0.288
Modified linear 2D	1.50	0.319	1.50	0.351	1.70	0.384

5.3 BER performance with unknown doppler frequency

The proposed method is tested with the assumption of unknown doppler frequency at the receiver to evaluate the performance of the proposed method for practical applications.

This is performed by having fixed doppler frequency correlation values at the interpolator while changing the multipath channel profile and the mobile station's velocity. Figures 5.4, 5.5 and 5.6 show the BER performance obtained for the modified and the conventional 2D method under different channel models.

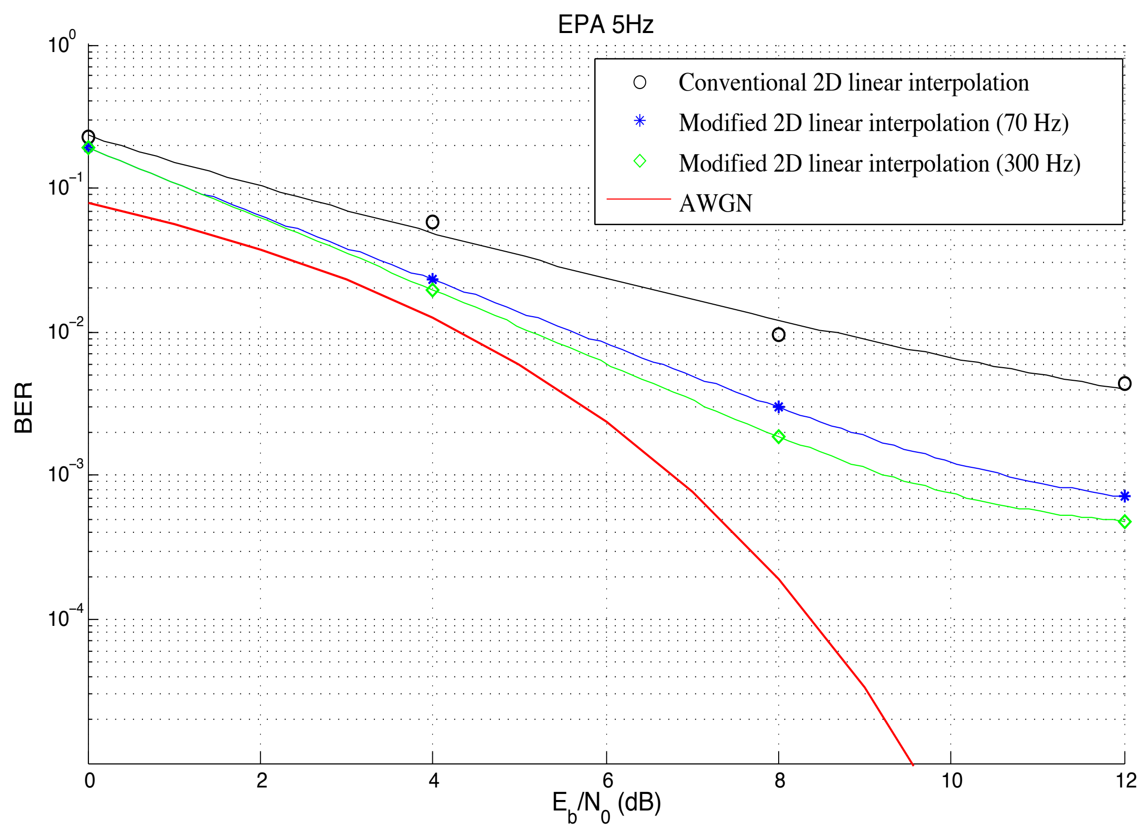

Figure 5.4: BER performance under the EPA 5Hz channel model without the knowledge of $\mathbf{F_d^{max}}$ at the receiver

As noticed from figure 4.4, the Jakes' time correlation relations for both the 70 Hz and the 300 Hz are close to each other, which would result in having close results when using any of the proposed correlation values for the different channel models; this significant result makes the proposed interpolation robust to any change of the mobile velocity.

Using the 70 Hz correlation values at E_b/N_0 of 12 dB gives BERs of 0.06%, 0.6% and 2.5% for EPA 5Hz, EVA 70Hz and ETU 300Hz channel models, respectively. Meanwhile using the 300 Hz correlation values at the same E_b/N_0 gives BERs of 0.045%, 0.5% and 2.0% for EPA 5Hz, EVA 70Hz and ETU 300Hz, respectively.

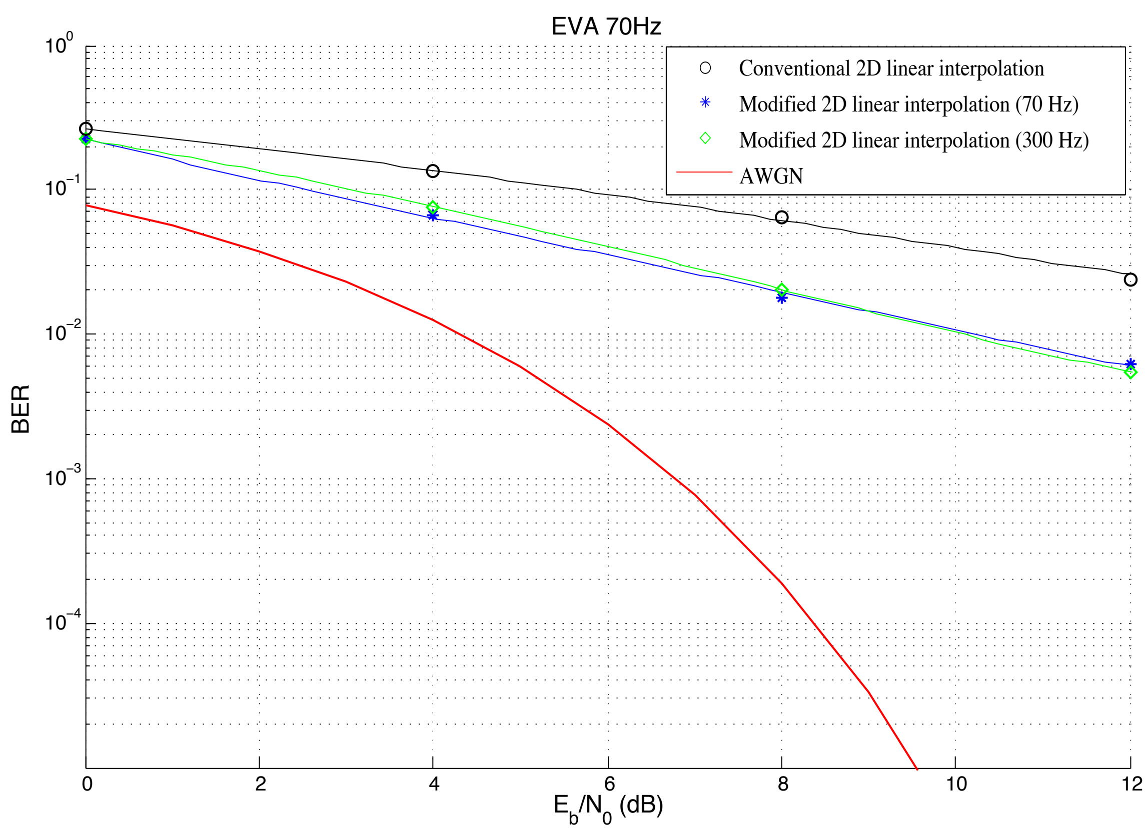

Figure 5.5: BER performance under the EVA 70Hz channel model without the knowledge of $\mathbf{F}_{\mathbf{d}}^{\mathbf{max}}$ at the receiver

It can be noticed that using the correlation values of the 300 Hz doppler frequency gives slightly better BER performance for most of the channels, which means that we can use the 300 Hz correlation values in the proposed method without the need to know the actual mobile velocity.

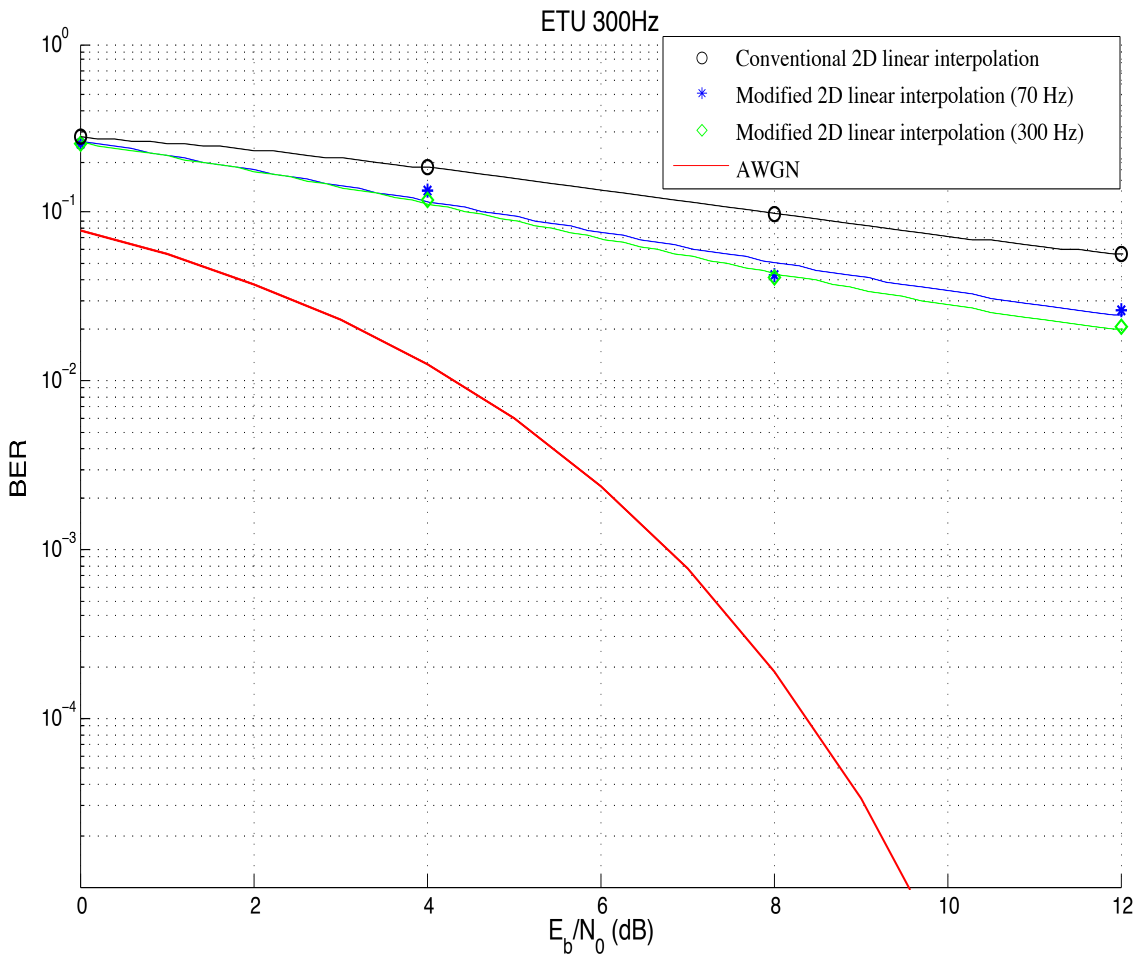

Figure 5.6: BER performance under the ETU 300Hz channel model without the knowledge of $\mathbf{F_d^{max}}$ at the receiver

Such a result gives a significant advantage for the proposed interpolation method over the conventional one, since the BER performance is insensitive to some extent to the change of the mobile velocity which results in reducing the number of assumptions that need to be made at the receiver which makes the proposed method more practical.

Table 5.3 compares the required processing time for the conventional 2D method and the proposed method under the assumption of unknown doppler frequency at the receiver at E_b/N_0 = 8 dB.

The processing time will not change for the conventional 2D method since it does not rely on the knowledge of the doppler frequency.

Since the proposed method takes advantage of the Jakes' correlation values and lowers the computational complexity by having fixed matrices representing the correlation values at the interpolator, the processing time for the three channel models would be very close.

For the modified method with the 70 Hz correlation values, an increase of 25.9% is needed for the processing time compared to the conventional 2D method for the ETU 300Hz channel.

An increase of 28.5% is required when using the modified method with the 300 Hz correlation values for the EPA 5Hz channel model and 53.8% when it is used under the EVA 70Hz channel.

Table 5.3: Processing time comparison between the proposed methods and the conventional 2D method without the knowledge of $\mathbf{F_d^{max}}$ at the receiver

	EPA 5Hz channel		EVA 70Hz channel		ETU 300Hz channel	
Method	Time percentage (%)	Time/call (ms)	Time percentage (%)	Time/call (ms)	Time percentage (%)	Time/call (ms)
Conventional 2D	0.950	0.223	1.10	0.255	1.10	0.288
Modified 2D (70 Hz)	1.50	0.319	1.50	0.351	1.60	0.363
Modified 2D (300 Hz)	1.40	0.287	1.90	0.393	1.70	0.384

5.4 One slot interpolation vs. one subframe interpolation performance

As stated in chapter four, the OFDM symbols at the edge of a slot have poor channel estimates. The one subframe proposed 2D interpolation solution performance is compared to the one slot interpolation in terms of BER performance and required processing time.

Figures 5.7, 5.8 and 5.9 show the BER performance comparison carried out for the three channel models.

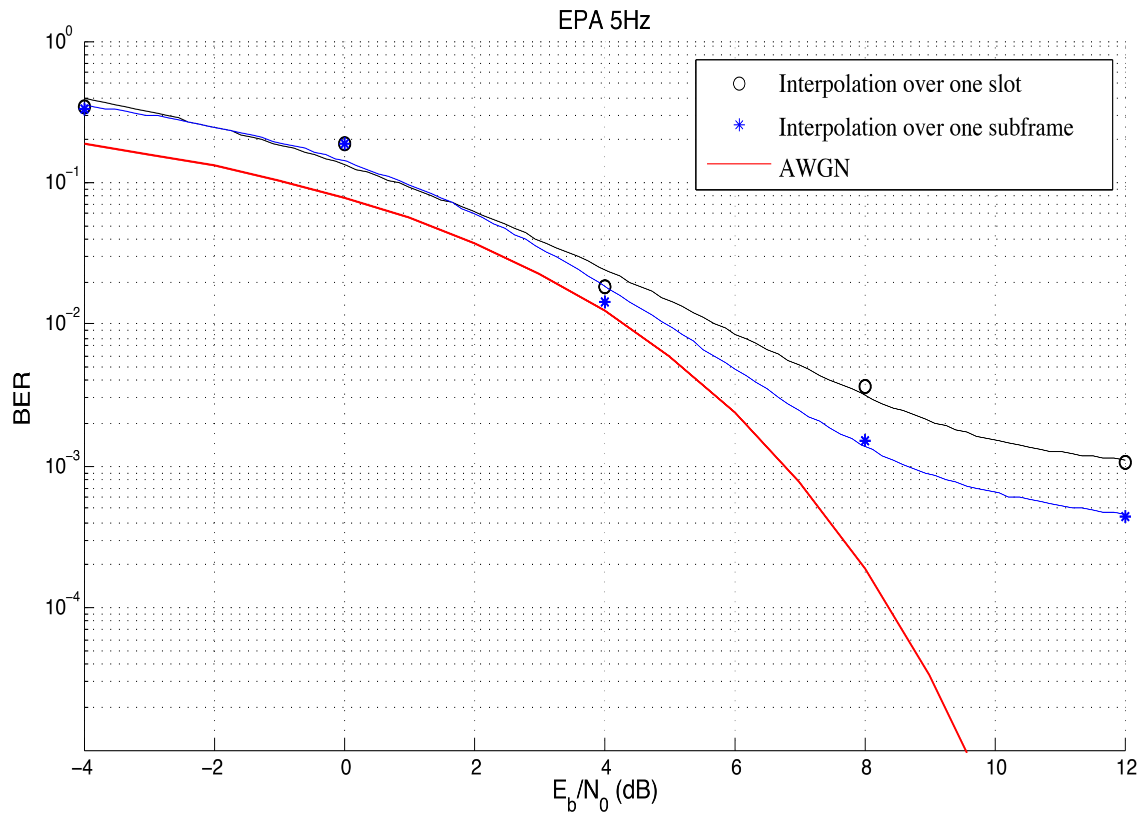

Figure 5.7: BER performance comparison between one slot and one subframe interpolation under the EPA 5Hz channel model

A BER improvement is obtained for all the three channel models but with different significance. Under the EPA 5Hz channel model, the improvement in the BER performance is obtained for all the ranges of the E_b/N_0.

For the EVA 70Hz channel model, the BER improvement can be noticed approximately after E_b/N_0 of 4 dB.

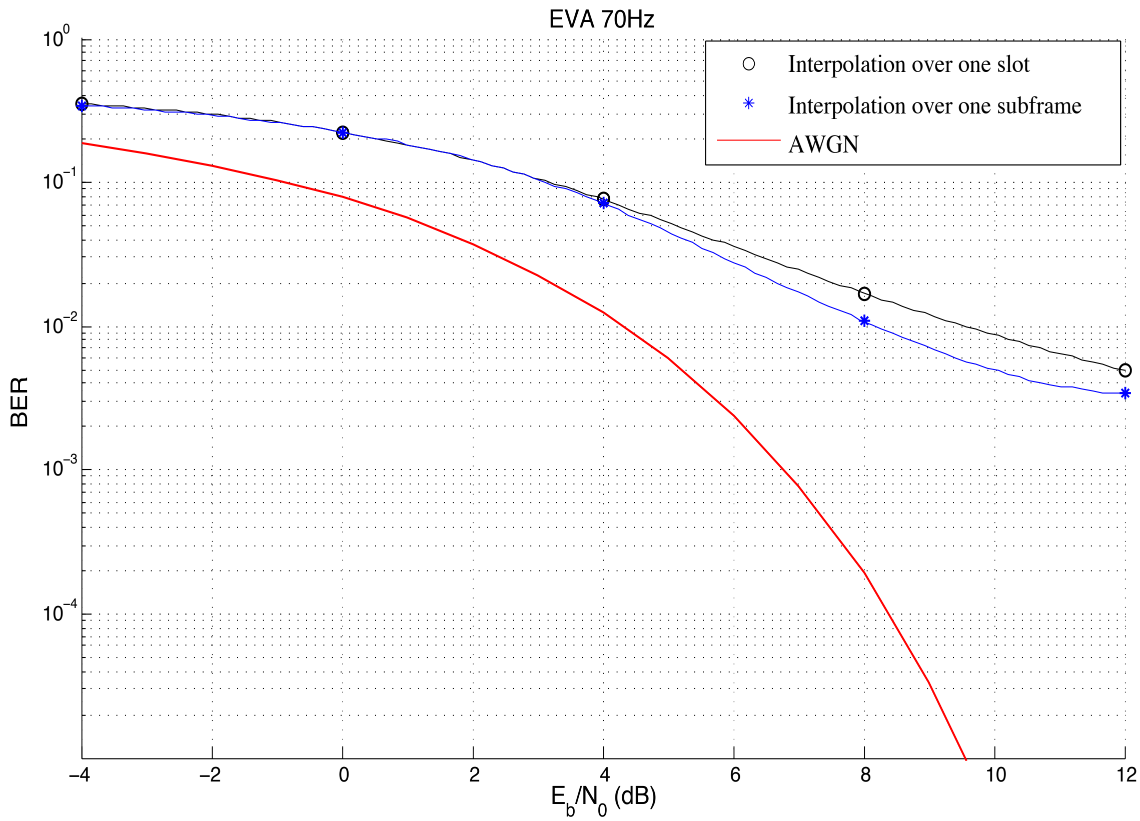

Figure 5.8: BER performance comparison between one slot and one subframe interpolation under the EVA 70Hz channel model

The significant improvement is gained when using the proposed solution for the ETU 300Hz channel model for E_b/N_0 above 5 dB. Since the ETU 300Hz channel is the fastest considered time-varying channel model in the test, the OFDM symbols at the edge of a transmitted slot will have the poorest channel estimates when using the one slot interpolation method; for that, these OFDM symbols benefit the most from the use of the one subframe proposed interpolation solution to improve the obtained channel estimates under the fast time-varying channel, and improve the overall BER performance as shown in figure 5.9.

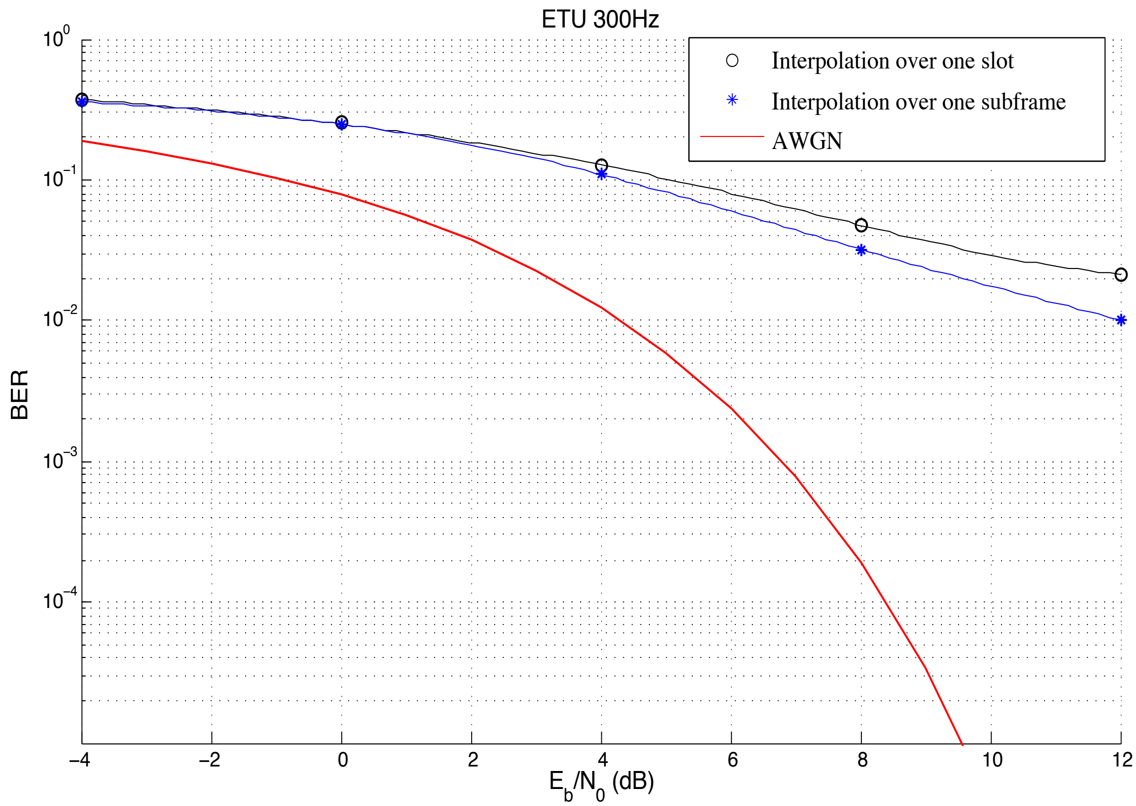

Figure 5.9: BER performance comparison between one slot and one subframe interpolation under the ETU 300Hz channel model

The needed processing times per call for the one slot and the one subframe interpolation are shown in table 5.4.

The processing time for the one subframe interpolation is increased in general more than 100% of the needed processing time for the one slot method, since it introduces a delay of one slot per call as each slot's channel estimates need to be stored to be used by the next processed slot. An additional delay is also introduced when performing the modified 2D interpolation method between the two slots in one subframe.

Table 5.4: Processing time comparison between the one slot and the one subframe interpolations

	EPA 5Hz channel		EVA 70Hz channel		ETU 300Hz channel	
Method	Time percentage (%)	Time/call (ms)	Time percentage (%)	Time/call (ms)	Time percentage (%)	Time/call (ms)
One slot interpolation	1.50	0.319	1.50	0.351	1.60	0.363
One subframe interpolation	1.90	0.767	2.16	0.789	2.23	0.806

The processing time per call for the one subframe and the one slot interpolation methods is almost the same when used under the three channel models; this is due to the advantage of having a fixed correlation matrix at the interpolator.

An increase of 140% of the required processing time is needed for the subframe interpolation under the EPA 5Hz channel compared to the one slot method, while 124% more processing time is needed under the EVA 70Hz and an increase of 122% under the ETU 300Hz channel.

At the end, the proposed method is tested for different mobile velocities using the 70 Hz correlation values as fixed values at the interpolator to see the limits of the proposed method when the mobile velocity increases.

Figure 5.10 shows the BER at 10 dB for different doppler frequencies that represent different mobile velocities for both the conventional and the proposed 2D linear interpolation methods.

It can be noticed that the slope of the BER increases after the doppler frequency of 300 Hz by almost three times of the BER slope before that doppler frequency for the proposed method.

This shows that the proposed solution, to overcome the need of making the assumption of the knowledge of the doppler frequency at the receiver, is efficient up to certain doppler frequencies.

The maximum doppler frequency at which the receiver can adequately operate depends on the BER floor tolerance of the entire communication system and the expected outcome quality from the interpolator.

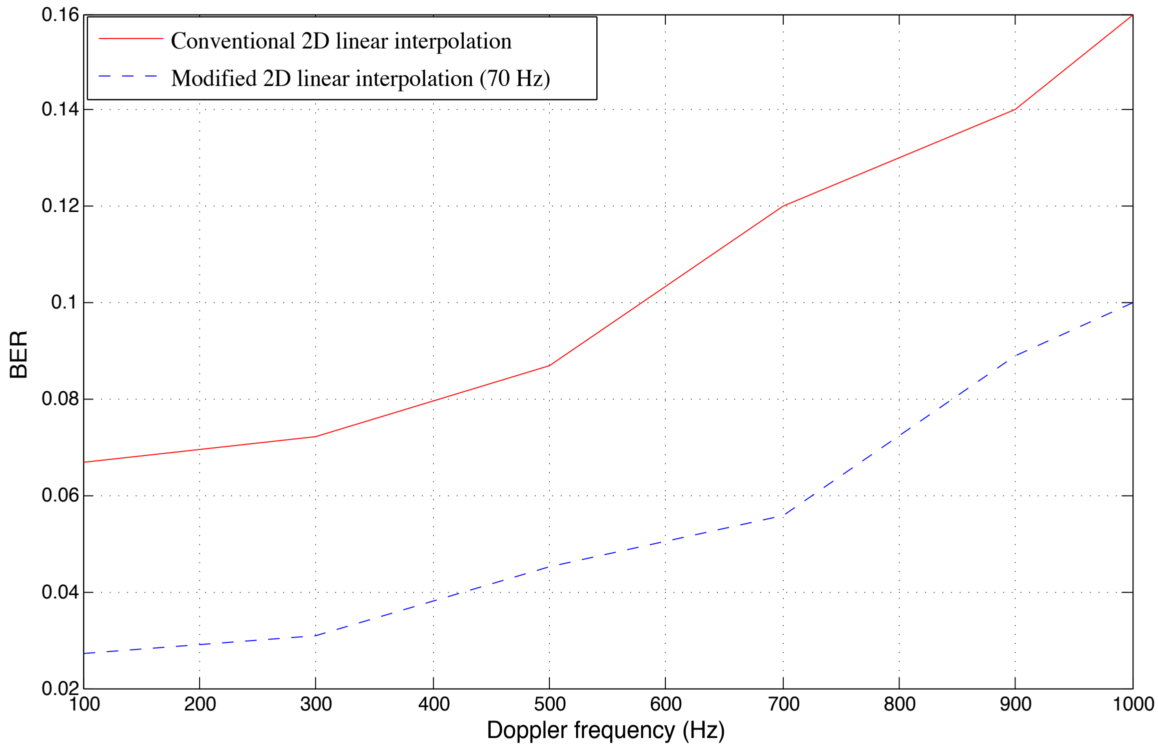

Figure 5.10: BER performance at 10 dB of the proposed method with various doppler frequencies

Chapter 6

Summary and future work

6.1 Summary of the proposed work

This thesis provides an innovative low-complexity approach for channel estimation and interpolation for mobile stations under fast time-varying LTE channel models. A significant BER performance improvement is achieved without the need to perform many complex operations at the receiver. Such an estimator would be efficient for mobiles operating at high velocities while using real-time interactive applications.

The proposed method utilizes the Jakes' correlation relationship across the OFDM symbols of a transmission frame to increase the number of dependencies used for the channel interpolation of the data subcarriers.

The BER performance of the proposed approach is obtained for the LTE channel models for different mobile velocities with the assumption of the knowledge of the doppler frequency at the receiver for the first part of the test (section 5.2) and with the assumption of unknown doppler frequency at the receiver for the second part (section 5.3) to simulate practical situations, where most of the time, the channel statistics are not available at the receiver.

The processing time required for the proposed method is compared to the processing time needed for the conventional 2D linear method, and showed an acceptable increase in the required processing time of 33.2% for the ETU 300Hz channel model while improving the BER performance from 6% to 2%.

One major advantage of the proposed method is the insensitivity to the change in the mobile velocity to some extent; such an advantage makes the proposed channel estimator more practical for different transmission environments and robust to any change in the channel statistics.

To improve the channel estimates at the edges of the transmitted slots and improve the overall BER performance, interpolation over one subframe is proposed instead of interpolation over one slot at a time.

6.2 Future work

The LTE-based system that is used in the thesis can be developed to include more aspects of the LTE downlink transmission such as the use of the channel state parameters from the mobile station at the base station. These parameters includes: Channel Quality Indicator (CQI), Pre-coding Matrix Indicator (PMI) and Rank Indicator (RI) [16].

The proposed method can be developed for MIMO-LTE based systems and for multiple users using the channel dependent scheduling and rate adaptation of the LTE transmission specifications.

More aspects and technologies of the LTE-Advanced standards can be added to the system to test how adaptive the proposed method can be to different technologies; such aspects can include the carrier aggregation feature of the LTE-Advanced systems, the extended multi-antenna transmission feature that supports up to eight transmission layers simultaneously and the adaptive modulation and coding rate at the transmitter [16, 18].

Due to the relatively long processing time required for the interpolation over one subframe, future research may consider the development of an advanced interpolation method to overcome this issue.

The proposed method can be tested for different LTE transmission modes for future work; that may include the use of pre-coding matrices and the layer mapping technique.

References

1. M. Yalcin, A. Akan, and H. Dogan, "Low-Complexity Channel Estimation for OFDM Systems in High-Mobility Fading Channels", *Turk Journal on Electrical Engineering and Computer Science*, vol. 20, no. 4, 2012.
2. J. Lee, J. Han, and J. Zhang, "MIMO Technologies in 3GPP LTE and LTE-Advanced", *EURASIP Journal on Wireless Communications and Networking*, vol. 2009, no. 302092, 2009.
3. F. Weng, C. Yin, and T. Luo, "Channel Estimation for The Downlink of 3GPP-LTE Systems", *2nd IEEE International Conf. on Network Infrastructure and Digital Content*, Beijing, China, pp. 1042-1046, Sept. 24-26, 2010.
4. Z. Tang, R. Cannizzaro, G. Leus, and P. Banelli, "Pilot-Assisted Time-Varying Channel Estimation for OFDM Systems", *IEEE Trans. on Signal Processing*, vol. 55, no. 5, pp. 2226-2238, May 2007.
5. K. Rajeswari et al., "Performance Analysis of Pilot Aided Channel Estimation Methods for LTE System in Time-Selective Channels", *5th International Conf. on Industrial and Information Systems*, Mangalore, India, pp. 113-118, July 29-Aug. 1st, 2010.
6. H. Nguyen-Le, T. Le-Ngoc, and C. Chung Ko, "Turbo Joint Decoding, Synchronization and Channel Estimation for Coded MIMO-OFDM Systems", *ICC Proc.*, Beijing, China, pp. 4366-4370, May 19-23, 2008.

7. H. Hafez, Y. A. Fahmy, and M. M. Khairy, "Iterative Channel Estimation and Turbo Decoding for OFDM Systems", *7th IEEE International Conf. on (WiMob)*, Wuhan, China, pp. 428-432, Oct. 11-12, 2011.

8. S. G. Kang, Y. M. Ha, and E. K. Joo, "A Comparative Investigation on Channel Estimation Algorithms for OFDM in Mobile Communications", *IEEE Trans. on Broadcasting*, vol. 49, no. 2, pp. 142-149, June 2003.

9. C. R. N. Athaudage and A. D. S. Jayalath, " Low-Complexity Channel Estimation for Wireless OFDM Systems", *14th IEEE Proc. on Personal, Indoor and Mobile Radio Communications*, Beijing, China, pp. 521-525, Sept. 7-10, 2003.

10. M. F. Rabbi, S. W. Hou, and C. C. Ko, "High Mobility Orthogonal Frequency Division Multiple Access Channel Estimation Using Basis Expansion Model", *IET Communications*, vol. 4, no. 3, pp. 353-367, Feb. 12, 2010.

11. Y. E. Shehadeh and S. Sezginer, "Fast Varying Channel Estimation in Downlink LTE Systems", *21st IEEE Symposium on Personal, Indoor and Mobile Radio Communications*, Istanbul, Turkey, pp. 608-613, Sept. 26-30, 2010.

12. N. M. Idrees, W. Haselmayr, M. Petit and A. Springer, "Complexity Reduction for Time Variant Channel Estimation in 3GPP LTE Downlink", *11th International Conf. on Telecommunications*, Graz, Austria, pp. 47-50, June 15-17, 2011.

13. N. M. Idrees, W. Haselmayr, D. Schellander and A. Springer, "Time Variant Channel Estimation Using a Modified Complex Exponential Basis Expansion Model in LTE-OFDM Systems", *21st IEEE Symposium on Personal, Indoor and Mobile Radio Communications*, Istanbul, Turkey, pp. 603-607, Sept. 26-30, 2010.

14. L. A. M. R. D. Temino, C. N. I. Manchon, C. Rom, T. B. Sorensen and P. Mogensen, "Iterative Channel Estimation with Robust Wiener Filtering in LTE Downlink", *Vehicular Technology Conf.*, Calgary, Canada, pp. 1-5, Sept. 21-24, 2008.

15. 3GPP TS 36.212 v10.4.0: " Evolved Universal Terrestrial Radio Access (E-UTRA); Multiplexing and Channel Coding", Jan. 2012.

16. 3GPP TS 36.213 v10.4.0: " Evolved Universal Terrestrial Radio Access (E-UTRA); Physical Layer Procedures", Jan. 2012.

17. 3GPP TS 36.101 v10.1.1: " Evolved Universal Terrestrial Radio Access (E-UTRA); User Equipment (UE) Radio Transmission and Reception", Jan. 2011.

18. 3GPP TS 36.211 v10.4.0: " Evolved Universal Terrestrial Radio Access (E-UTRA); Physical Channels and Modulation", Jan. 2012.

19. E. Dahlman, S. Parkvall and J. Skold, 4G LTE/LTE-Advanced for Mobile Broadband, Academic Press, 2011.

20. R. V. Nee and R. Prasad, OFDM for Wireless Multimedia Communications, Artech House, 2000.

21. W. C. Jakes, Microwave Mobile Communication, Wiley, New York, 1974.

22. Y. T. Desta, J. Tao and W. Zhang, " Review on Selected Channel Estimation Algorithms for Orthogonal Frequency Division Multiplexing System", *Information Technology Journal*, 10: 914-926, 2011.

23. L. Kewen and Xingke, " Research of MMSE and LS Channel Estimation in OFDM Systems", *2nd International Conf. on Information Science and Engineering*, Hangzhou, China, pp. 2308-2311, Dec. 4-6, 2010.

24. X. Dong, W. S. Lu and A. C. K. Soong, " Linear Interpolation in Pilot Symbol Assisted Channel Estimation for OFDM", *IEEE Trans. on Wireless Communications*, vol. 6, no. 5, pp. 1910-1920, May 2007.

25. S. Coleri, M. Ergen, A. Puri and A. Bahai, " Channel Estimation Techniques Based on Pilot Arrangement in OFDM systems", *IEEE Trans. on Broadcasting*, vol. 48, no. 3, pp. 223-229, Sept. 2002.

26. J. Rinne and M. Renfors, " Pilot Spacing in Orthogonal Frequency Division Multiplexing Systems on Practical Channels", *IEEE Trans. on Consumer Electronics*, vol. 42, no. 4, pp. 959-962, Nov. 1996.

27. C. R. N. Athandage and A. D. S. Jayalath, " A Novel RMS Delay-Spread Estimation Technique for Wireless OFDM Systems", *Proc. of the 2003 Joint Conf. of the Fourth International Conf. on Information, Communications and Signal Processing, 2003 and Fourth Pacific Rim Conf. on Multimedia*, Orchard, Singapore, pp. 626-630, Dec. 15-18 2003.

28. X. Dai, W. Zhang, J. Xu, J. E. Mitchell and Y. Yang, " Kalman Interpolation Filter for Channel Estimation of LTE Downlink in High Mobility Environments", *EURASIP Journal on Wireless Communications and Networking*, vol. 2012, no. 1, July 25, 2012.

Appendices

A Simulink blocks setup

A.1 QAM mapping setup

The QAM takes binary digits and maps it to complex-valued symbols I and Q as shown in tables B.1 and B.2 for the 4-QAM and 16-QAM schemes [18].

Table A.1: 4-QAM mapping

	00	01	10	11
I	$1/\sqrt{2}$	$1/\sqrt{2}$	$-1/\sqrt{2}$	$-1/\sqrt{2}$
Q	$1/\sqrt{2}$	$-1/\sqrt{2}$	$1/\sqrt{2}$	$- 1/\sqrt{2}$

Table A.2: 16-QAM mapping

	I	Q
0000	$1/\sqrt{10}$	$1/\sqrt{10}$
0001	$1/\sqrt{10}$	$3/\sqrt{10}$
0010	$3/\sqrt{10}$	$1/\sqrt{10}$
0011	$3/\sqrt{10}$	$3/\sqrt{10}$

0100	$1/\sqrt{10}$	$-1/\sqrt{10}$
0101	$1/\sqrt{10}$	$-3/\sqrt{10}$
0110	$3/\sqrt{10}$	$-1/\sqrt{10}$
0111	$3/\sqrt{10}$	$-3/\sqrt{10}$
1000	$-1/\sqrt{10}$	$1/\sqrt{10}$
1001	$-1/\sqrt{10}$	$3/\sqrt{10}$
1010	$-3/\sqrt{10}$	$1/\sqrt{10}$
1011	$-3/\sqrt{10}$	$3/\sqrt{10}$
1100	$-1/\sqrt{10}$	$-1/\sqrt{10}$
1101	$-1/\sqrt{10}$	$-3/\sqrt{10}$
1110	$-3/\sqrt{10}$	$-1/\sqrt{10}$
1111	$-3/\sqrt{10}$	$-3/\sqrt{10}$

A.2 Pseudo random sequence generation

The pilot symbols in LTE are generated using the pseudo random sequences. The sequences are defined by a length of 31 gold sequence [18]. The output sequence y(n) of length P, where n = 0, 1, …, P-1, is defined as:

$$y(n) = \left(x_1(n + N_c) + x_2(n + N_c)\right) \bmod 2 \tag{A.1}$$

$$x_1(n + 31) = (x_1(n + 3) + x_1(n)) \bmod 2 \tag{A.2}$$

$$x_2(n + 31) = (x_2(n + 3) + x_2(n + 2) + x_2(n + 1) + x_2(n)) \bmod 2, \tag{A.3}$$

where N_c = 1600 and the first sequence shall be initialized with $x_1(m)$ = 0 for m = 0, 1, …, 30.

B The proposed algorithm derivations

B.1 Doppler spectrum and time correlation function

The doppler spectrum gives an intuition into the rate of change of the wireless communication channel.

The doppler frequency F_d is expressed as:

$$F_d = \frac{v \cos\theta}{c} F_c, \tag{B.1}$$

where F_c is the carrier frequency, v is the mobile velocity, c represents the speed of light and θ is the angle of arrival at the receiver of the radio waves, which is assumed to be uniformly distributed.

To compute the doppler spectrum, the correlation function is needed. If we have two channel coefficients $a_i(x)$ at time t and $t + \Delta t$ of the i^{th} path as follows:

$$a_i(t) = a_i\, e^{-j2\pi f T_i}\, e^{j2\pi F_d t} \tag{B.2}$$

$$a_i(t+\Delta t) = a_i\, e^{-j2\pi f T_i}\, e^{j2\pi F_d (t+\Delta t)} \tag{B.3}$$

The correlation function R of the time interval Δt is defined as:

$$R(\Delta t) = E\{\, a_i(t)\, a_i^*(t+\Delta t)\, \} \tag{B.4}$$

$$R(\Delta t) = E\{\, |a_i|^2\, e^{-j2\pi F_d \Delta t}\, \} \tag{B.5}$$

With normalized power, $|a_i|^2 = 1$, the correlation function can be written as:

$$R(\Delta t) = E\{\, e^{-j2\pi F_d \Delta t}\, \} \tag{B.6}$$

$$R(\Delta t) = E\{\, e^{-j2\pi \left(\frac{v \cos\theta}{c} F_c\right)\Delta t}\, \} \tag{B.7}$$

when $\theta = 0$, $F_d = F_d^{max}$, where $F_d^{max} = \frac{v}{c} F_c$.

The correlation function in terms of F_d^{max} can be expressed as:

$$R(\Delta t) = E\{\, e^{-j2\pi F_d^{max} \cos\theta\ \Delta t}\, \} \tag{B.8}$$

Since θ is uniformly distributed between 0 and π, the correlation function can be written as:

$$R(\Delta t) = \int_0^{\pi} \frac{1}{\pi}\, e^{-j2\pi F_d^{max} \cos\theta\ \Delta t}\, d\theta \tag{B.9}$$

$$R(\Delta t) = J_0(2\pi\, F_d^{max} \Delta t) \tag{B.10}$$

B.2 The proposed interpolation algorithm

The received signal y at the n^{th} OFDM symbol and the k^{th} subcarrier can be written as:

$$y(n,k) = h(n,k)\, x(n,k) + w(n,k), \tag{B.11}$$

where h(n , k) is the channel frequency response, x(n, k) is the transmitted signal and w(n, k) represents the additive white Gaussian noise.

The obtained channel estimate $\widehat{H}$ at the pilot symbols at the p^{th} OFDM symbol and q^{th} subcarrier is expressed as follows:

$$\widehat{H}(p,q) = \frac{y(p,q)}{x(p,q)}, \tag{B.12}$$

where p represents the OFDM symbol with the pilot symbols and q denotes the subcarrier index for the pilot symbols. The channel frequency at the data subcarriers is estimated then by interpolating the channel estimates at neighboring pilot symbols and can be generally expressed as:

$$\widehat{H}(n,k) = w(n,p;k,q)\, \widehat{H}(p,q), \tag{B.13}$$

where $w(n,p;k,q)$ is a weighting function associated with the particular interpolation method used, and it depends on using the channel estimates at the pilot symbols.

To obtain the channel estimates of the data symbols, $\widehat{H}(F_1)$, $\widehat{H}(F_2)$, ..., $\widehat{H}\left(F_{N_{sp}}\right)$, linear interpolation is first applied at the subcarriers between each of the two pilot symbols in the first and the fifth OFDM symbol, using equation (4.6) as follows:

$$\widehat{H}(F_k) = \left(\frac{\widehat{H}(F_{q+1}) - \widehat{H}(F_q)}{F_{q+1} - F_q}\right)(F_k - F_q) + \widehat{H}(F_q), k = 0, 1, 2, \dots, N_{sp}. \tag{B.14}$$

where N_{sp} is the number of subcarriers between pilots. Observe $\widehat{H}(F_0) = \widehat{H}(F_q)$.

An extrapolation method using equation (4.7) is applied for the data symbols outside the pilot's range in the first and the fifth OFDM symbols as follows:

$$\widehat{H}(F_k) = \left(\frac{\widehat{H}(F_q) - \widehat{H}(F_{q-1})}{F_q - F_{q-1}}\right)(F_k - F_q) + \widehat{H}(F_q) \tag{B.15}$$

At this point, the channel estimates for all the subcarriers of the first and the fifth OFDM symbols are available and they can be considered as secondary pilots to obtain the channel estimates for the remaining OFDM symbols in the transmission slot.

Linear interpolation is applied between the first and the fifth OFDM symbols at each subcarrier to obtain the channel estimates for the second, the third and the fourth OFDM symbols using equation (4.6) as follows:

$$\widehat{H}(n, k) = \left(\frac{\widehat{H}(5, k) - \widehat{H}(1, k)}{5T_s - T_s}\right)(n\,T_s - T_s) + \widehat{H}(1, k) \tag{B.16}$$

Linear extrapolation is applied also to obtain the channel estimates at each subcarrier for the sixth and the seventh OFDM symbols using equation (4.7) as follows:

$$\widehat{H}(n, k) = \left(\frac{\widehat{H}(5, k) - \widehat{H}(1, k)}{5T_s - T_s}\right)(nT_s - 5T_s) + \widehat{H}(5, k) \tag{B.17}$$

At this point of the algorithm, the full channel estimates matrix for all data symbols is available. The correlation relationship modifications are applied next to improve the obtained channel estimates.

The channel estimates are separated into real and imaginary parts and the time correlation function is solved for n = T_s, $2T_s$ and $3T_s$, where the frequency correlation function is solved for k = Δf, 2Δf and 3Δf.

The channel estimates of the REs between the pilots as in figure 4.3 are weighted by the corresponding correlation values in an averaging way and the choice of p and q depends on the which pilot estimate is used as shown in figure 4.3 for different REs. This can be expressed as follows:

$$\mathrm{Real}[\widehat{H}(n,k)] = \frac{\mathrm{Real}[H(p,q)]\, R_t(n) + \mathrm{Real}[H(n,k)]}{2} \tag{B.18}$$

$$\mathrm{Imag}[\widehat{H}(n,k)] = \frac{\mathrm{Imag}[H(p,q)]\, R_f(k) + \mathrm{Imag}[H(n,k)]}{2} \tag{B.19}$$

$$\widehat{H}(n,k) = \mathrm{Real}\left[\widehat{H}(n,k)\right] + j\, \mathrm{Imag}[\widehat{H}(n,k)] \tag{B.20}$$

$\widehat{H}(n,k)$ is fed after to a gain and phase compensation stage to inverse the effect of the time-varying channel.

C Embedded MATLAB code

C.1 OFDM modulator code

```
function y = OFDMmod(in)
%%%%%%%%%%%%%%%%%%%%%%%%%%%%%%%%%%%%%%%%%%%%%%%%%%
% Function for OFDM modulation process at the transmitter
% Assumes transmitting one slot of data per time step
% Assumes SISO transmission
```

```
% Data created: December 2012.
% Disclaimer:     I am not liable for damages resulting from the use of
                  this program.
%%%%%%%%%%%%%%%%%%%%%%%%%%%%%%%%%%%%%%%%%%%%%%%%%%


[len, numSymb] = size(in);
N = 128; % Number of subcarriers
cpLen0 = 10; cpLenR = 9; % Different CP length across the OFDM symbols
slotLen = (N*7 + cpLen0 + cpLenR*6); %Length of one slot
tmp = complex(zeros(N, numSymb));
% Pack data and reorder
tmp(N/2-len/2+1:N/2, :) = in(1:len/2, :);
tmp(N/2+2:N/2+1+len/2, :) = in(len/2+1:len, :);
% IFFT operation with gain scale
x = ifft(tmp, N, 1);
x = x.*(sqrt(N)*sqrt(N/len));
% Add cyclic prefix per OFDM symbol and serialize over the slot
y = complex(zeros(slotLen, 1));


% First OFDM symbol
y((1:cpLen0), :) = x((N-cpLen0+1):N, 1);
y(cpLen0+(1:N), :) = x(1:N, 1);


% Next 6 OFDM symbols for a normal CP
for k = 1:6
y(cpLen0+k*N+(k-1)*cpLenR+(1:cpLenR), :) = x(N-cpLenR+1:N, (k+1);
y(cpLen0+k*N+k*cpLenR+(1:N), :) = x(1:N, k+1);
end
```

C.2 OFDM de-modulator code

```
function y = OFDMdemod(in)

%%%%%%%%%%%%%%%%%%%%%%%%%%%%%%%%%%%%%%%%%%%%%%%%%%

% Function for OFDM de-modulation process at the receiver

% Assumes receiving one slot of data per time step

% Assumes SISO transmission

% Data created: December 2012.

% Disclaimer:     I am not liable for damages resulting from the use of
                  this program.

%%%%%%%%%%%%%%%%%%%%%%%%%%%%%%%%%%%%%%%%%%%%%%%%%%


N = 128;

cpLen0 = 10; cpLenR = 9;

slotLen = (N*7 + cpLen0 + cpLenR*6);

tmp = complex(zeros(N, 7)); % OFDM symbols/slot = 7

% Remove CP


% First OFDM symbol

tmp(:, 1 ) = in(cpLen0 + (1: N), :);

% Next 6 OFDM symbols

for k = 1:6

    tmp(:, k+1) = in(cpLen0+k* N +k* cpLenR + (1: N), :);

end


% FFT operation with gain scale

x = fft(tmp, N, 1);

x =  x./(sqrt(N)*sqrt(N /72)); % Data tones = 6 Rbs*12 subcarriers
```

```
% For one slot
y = complex(zeros(72, 7));

% Unpack data and reorder
y(1:(72/2), :) = x(N/2-72/2+1:N/2, :);
y(72/2+1:72, :) = x(N/2+2:N/2+1+72/2, :);
end
```

C.3 LTE channel setup

```
function y = LTEChan(in)
%%%%%%%%%%%%%%%%%%%%%%%%%%%%%%%%%%%%%%%%%%%%%%%%%%
% Function to generate the impulse response for LTE channel models and
% filter the data through it.
% Assumes SISO transmission
% Data created: December 2012.
% Disclaimer:      I am not liable for damages resulting from the use of
                   this program.
%%%%%%%%%%%%%%%%%%%%%%%%%%%%%%%%%%%%%%%%%%%%%%%%%%

coder.extrinsic('rayleighchan');
x = complex(zeros(size(in, 1), 1));
% simulation parameters
Tx = 1;
Rx = 1;
SamplingFreq = 1920000;
SampleTime = 1/ SamplingFreq;
EPAPathDelays = [0 30 70 90 110 190 410]*1e-9;
```

```
EPAPathGains  = [0 -1 -2 -3 -8 -17.2 -20.8];

EVAPathDelays = [0 30 150 310 370 710 1090 1730 2510]*1e-9;

EVAPathGains  = [0 -1.5 -1.4 -3.6 -0.6 -9.1 -7 -12 -16.9];

ETUPathDelays = [0 50 120 200 230 500 1600 2300 5000]*1e-9;

ETUPathGains  = [-1 -1 -1 0 0 0 -3 -5 -7];


% Rayleigh channel setup

PathDelays          = ETUPathDelays;

AveragePathGains    = ETUPathGains;

MaximumDopplerShift = 300;


% Create the channel object

persistent chan;

if isempty(chan)

    chan = rayleighchan(SampleTime, MaximumDopplerShift, PathDelays,
AveragePathGains);

end


% Filter data through the Channel

x  = filter(chan, in);

y=x;

end
```

C.4 Modified 2D interpolation method code

```
function y = interpolation(pilot)

 %%%%%%%%%%%%%%%%%%%%%%%%%%%%%%%%%%%%%%%%%%%%%%%%%%

% Function to perform interpolation over the OFDM symbols
```

```
% Assumes transmitting one slot of data per time step
% Assumes SISO transmission
% Data created: January 2013.
% Disclaimer:     I am not liable for damages resulting from the use of
                  this program.
%%%%%%%%%%%%%%%%%%%%%%%%%%%%%%%%%%%%%%%%%%%%%%%%%%


coder.extrinsic (' interp1 ');
ChanEst= complex (zeros(72,7));
Sym1 = complex(zeros(1,72));ImagSym1 = complex(zeros(1,72));
Sym5 = complex(zeros(1,72));Sym2 = complex(zeros(1,72));
Sym6=complex(zeros(1,72));ImagSym5=complex(zeros(1,72));
Sym7=complex(zeros(1,72));initial = complex (zeros (1,7));
Sym4 =complex(zeros(1,72));
Rf70 = [0.9988-1j*0.0335 0.9956-1j*0.0675 0.99-1j*0.099 0.982-1j*0.132
0.97-1j*0.163];
Rt70 = [0.9998 0.999 0.9978 0.9961 0.9939 0.9912];
Rf300 = [ 0.9914-1j*0.0926 0.9663-1j*0.1805 0.9272-1j*0.2598 0.8775-
1j*0.3278 0.8210-1j*0.3834];
Rt300 = [0.9955 0.9822 0.9601 0.9601 0.9296 0.8912 0.8452];


% linear interpolation and extrapolation over the first OFDM symbol
u1 = [1 7 13 19 25 31 37 43 49 55 61 67]; % Pilot positions
uu = 1:1:72;
Sym1= interp1(u1,pilot(1:12),uu,'linear','extrap');


%Frequency correlation across the first OFDM symbol
ImagSym1 = imag(Sym1);
for i=[1 7 13 19 25 31 37 43 49 55 61];
```

```
 ImagSym1(i+1) = (Rf70(1)*ImagSym1(i) + conj(Rf70(5))*ImagSym1(i+6))/2;
 ImagSym1(i+2) = (Rf70(2)*ImagSym1(i) + conj(Rf70(4))*ImagSym1(i+6))/2;
 ImagSym1(i+3) = (Rf70(3)*ImagSym1(i) + conj(Rf70(3))*ImagSym1(i+6))/2;
 ImagSym1(i+4) = (Rf70(4)*ImagSym1(i) + conj(Rf70(2))*ImagSym1(i+6))/2;
 ImagSym1(i+5) = (Rf70(5)*ImagSym1(i) + conj(Rf70(1))*ImagSym1(i+6))/2;
end

for i=67
    ImagSym1(i+1) = Rf70(1)*ImagSym1(67);
    ImagSym1(i+2) = Rf70(2)*ImagSym1(67);
    ImagSym1(i+3) = Rf70(3)*ImagSym1(67);
    ImagSym1(i+4) = Rf70(4)*ImagSym1(67);
    ImagSym1(i+5) = Rf70(5)*ImagSym1(67);
end

% linear interpolation and extrapolation over the fifth OFDM symbol
u2 = [4 10 16 22 28 34 40 46 52 58 64 70]; % Pilot positions
Sym5 = interp1(u2,pilot(13:24),uu,'linear','extrap');

% Frequency correlation across the fifth OFDM symbol
ImagSym5=imag(Sym5);
for i=[4 10 16 22 28 34 40 46 52 58 64]
ImagSym5(i+1) = (Rf70(1)*ImagSym5(i) + conj(Rf70(5))*ImagSym5(i+6))/2;
ImagSym5(i+2) = (Rf70(2)*ImagSym5(i) + conj(Rf70(4))*ImagSym5(i+6))/2;
ImagSym5(i+3) = (Rf70(3)*ImagSym5(i) + conj(Rf70(3))*ImagSym5(i+6))/2;
ImagSym5(i+4) = (Rf70(4)*ImagSym5(i) + conj(Rf70(2))*ImagSym5(i+6))/2;
ImagSym5(i+5) = (Rf70(5)*ImagSym5(i) + conj(Rf70(1))*ImagSym5(i+6))/2;
end
```

```
ImagSym5(1)  = conj(Rf70(3))*ImagSym5(4);

ImagSym5(2)  = conj(Rf70(2))*ImagSym5(4);

ImagSym5(3)  = conj(Rf70(1))*ImagSym5(4);

ImagSym5(71) = Rf70(1)*ImagSym5(70);

ImagSym5(72) = Rf70(2)*ImagSym5(70);


% Linear interpolation across the OFDM symbols using the first and
% the fifth OFDM symbols channel estimates

for i=1:72

initial = interp1([1 5],[Sym1(i) Sym5(i)],[1:7],'linear','extrap');

ChanEst(i,:) = [ initial(1) initial(2) initial(3) initial(4) initial(5)
initial(6) initial(7) ];

End


% Apply correlation modifications in time and frequency from the first
% OFDM symbol's pilots across OFDM symbols 2,3 and 4.

imagChanEst= imag(ChanEst);realChanEst= real(ChanEst);

for i=u1

imagChanEst(i+1,2) = (Rf70(1)*imagChanEst(i,1)+imagChanEst(i+1,2))/2;

realChanEst(i+1,2) = (Rt70(1)*realChanEst(i,1)+realChanEst(i+1,2))/2;

imagChanEst(i+2,3) = (Rf70(2)*imagChanEst(i,1)+imagChanEst(i+2,3))/2;

realChanEst(i+2,3) = (Rt70(2)*realChanEst(i,1)+realChanEst(i+2,3))/2;

imagChanEst(i+3,4) = (Rf70(3)*imagChanEst(i,1)+imagChanEst(i+3,4))/2;

realChanEst(i+3,4) = (Rt70(3)*realChanEst(i,1)+realChanEst(i+3,4))/2;

end


% Apply correlation modifications in time and frequency from fifth OFDM
% symbol's pilots across OFDM symbols 4,3 and 2.

for i=u2
```

```
realChanEst(i,4)   = (Rt70(1)*realChanEst(i,5)+realChanEst(i,4))/2;
imagChanEst(i+1,3) = (Rf70(1)*imagChanEst(i,5)+imagChanEst(i+1,3))/2;
realChanEst(i+1,3) = (Rt70(2)*realChanEst(i,5)+realChanEst(i+1,3))/2;
imagChanEst(i+2,2) = (Rf70(2)*imagChanEst(i,5)+imagChanEst(i+2,2))/2;
realChanEst(i+2,2) = (Rt70(3)*realChanEst(i,5)+realChanEst(i+2,2))/2;
end

ChanEst = realChanEst+1j*imagChanEst;
y=ChanEst;
end
```

Vita

Candidate's full name: Ahmad El-Qurneh

University attended: Princess Sumaya University for Technology, Bachelor of Communication Engineering, 2011.